

ACKNOWLEDGEMENT

First of all, I am thankful to almighty Allah, the most merciful, for giving the strength and energy to accomplish this MS Thesis. I would like to express my sincere gratitude and thanks to my advisor Cdr. Dr. Tariq M. Khan for his encouragement, guidance and motivation through all the phases of this Thesis. I also like to thanks my GEC members Cdr. Dr. Faisal Amir, Dr. Muhammad Bilal Kadri and Cdr. Dr. Sajid Saleem for their comments, suggestions and time in reviewing this thesis.

I am also thankful to ICT R&D Pakistan and NDT Team of Pakistan International Airlines for providing support to accomplish this research work. The sincere thanks extended to my colleague Mr. Moez ul Hassan and NDT Research Team of PNEC for stimulating discussions

Finally, I would also like to oblige my family for their support, encouragement and understanding

ABSTRACT

Aerospace Non-destructive testing (NDT) is performed to determine the structural integrity of aircraft structure. The major components of the aircraft structure inspected include fuselage, wings, stabilizers, appendages, lap joints, multi layered structures etc. Determination of the integrity leads to flight worthiness assessment of the aircraft. Periodic testing of aircraft structures for damages such as corrosion and cracks is considered mandatory to ensure aircraft safety.

Need of hour is to develop in-country knowledge of NDT signal processing for damage detection and flaw sizing. This would reduce the dependence on the manufacturers input. In-house knowledge would also facilitate the decision makers to decide flight worthiness of the air craft in short period of time as wait period for recommendation from manufacturers can be eliminated.

Ultrasonic testing is used to detect and classify flaws on aerospace structures using modern signal processing techniques. Flaw diagnosis algorithms have been developed and subsequently implemented on the raw data acquired from actual aircraft structures. Time frequency analysis is conducted, due to non-stationary and non-linear nature of acquired ultrasonic signals from Aerospace structures. Results are compared based on Short Term Fourier Transform, Wavelet Transform and Hilbert Huang Transform and then applied for flaw detection and characterization. Intelligent feature extraction based on energy-frequency distribution at particular locations for diagnosis and crack estimation with the help for Hilbert Huang Transform is proposed in this research work

Table of Contents

ACKNOWLEDGEMENT	1
ABSTRACT.....	2
List of Figures	6
List of Tables	8
1 INTRODUCTION	10
1.1 Motivation.....	11
1.2 Objective	12
1.3 Outline of the Thesis	13
2 ULTRASONIC NON DESTRUCTIVE TESTING.....	14
2.1 Introduction to Ultrasonic Non-Destructive Testing.....	14
2.2 History of Ultrasonic.....	14
2.3 Advantages of UT	15
2.4 Disadvantages of UT.....	16
2.5 Aerospace Application of Ultrasonic Testing	16
3 EXPERIMENTAL SETUP AND TIME DOMAIN ANALYSIS	18
3.1 Ultrasonic NDT Setup.....	18
3.2 Interface of Ultrasonic Equipment and Data Format Analysis	19
3.3 Calibration Procedure	20
.....	22
3.4 Choice of Calibration Standards	22

3.5	Data Presentation	24
3.5.1	A-Scan (Amplitude Scan)	25
3.5.2	B-Scan (Cross Sectional View).....	27
3.5.3	C-Scan (Top View)	28
3.6	Time Domain Analysis Short Comings	29
4	FREQUENCY AND TIME FREQUENCY ANALYSIS.....	30
4.1	Introduction.....	30
4.2	Fourier Transform.....	30
4.2.1	Fourier Transform Based Classification and ROI Detection	32
4.3	Short Time Fourier Transform (STFT).....	33
4.4	Wavelet Transform	39
4.4.1	Continuous Wavelet Transform (CWT).....	39
4.4.2	Steps Involved in CWT Coefficients Calculation	41
4.4.3	Results Obtained Using CWT	42
4.5	Discrete Wavelet Transform	44
4.5.1	Sub Band Coding	45
4.5.2	DWT Result	46
4.6	Stationary Wavelet Transform.....	48
5	FLAW CHARACTERIZATION USING HILBERT HUANG TRANSFORM.....	50
5.1	Introduction.....	50
5.2	HHT Standard Process:.....	50
5.2.1	Empirical Mode Decomposition:	51

5.2.2	Steps Involved in EMD Calculation:	52
	54
5.3	Hilbert Transform	54
5.4	Data Acquisition for HHT.....	55
5.5	HHT Results and Discussion	57
6	CONCLUSION AND FUTURE WORK.....	62
6.1	Conclusion	62
6.2	Future Work.....	62
	References.....	63

List of Figures

Figure 3-1: Basic UT-NDT Setup.....	18
Figure 3-2: Acquiring Data Using Sonatest Data Management Software	20
Figure 3-3: Calibration Block for Thickness Calculation	22
Figure 3-4: Calibration block for testing at spindle	22
Figure 3-5: Ultrasonic Testing Transducers.....	24
Figure 3-6: Different Calibration Blocks	24
Figure 3-7 : Test Specimen used for Ultrasonic Testing.....	25
Figure 3-8: A-Scan plots of 25 Locations of the Test Specimen	26
Figure 3-9: Sample A-Scan, with initial pulse and back surface reflection marking.....	27
Figure 3-10: B-Scan or Cross Sectional View of Test Specimen	28
Figure 3-11 : C-Scan View of the Test Specimen.....	29
Figure 4-1: FFT at Healthy Location	31
Figure 4-2: FFT Spectrum at Cracked Location	31
Figure 4-3: FFT Spectrum at Cracked Location	32
Figure 4-4: STFT Spectrogram of Healthy Location.....	35
Figure 4-5: STFT Spectrogram Plot at Cracked Location	35
Figure 4-6: STFT spectrogram Plot at Cracked Location	35
Figure 4-7: Healthy Location Frequency Plots at particular Distance	36
Figure 4-8: Cracked Location STFT Spectrogram Plot Threads	37
Figure 4-9: Cracked Location STFT Spectrogram Threads.....	38
Figure 4-10: Scaling and Shifting Process using Mother Wavelet	40
Figure 4-11: Wavelet Spectrum of Healthy and Cracked Location. Top is Healthy Location Wavelet Spectrum and Bottom is Cracked Location Wavelet Spectrum.....	42
Figure 4-12: Wavelet Spectrum of Cracked Locations.....	43

Figure 4-13: Cracked Location Coefficient Plot at Scale Value 1 using Haar Wavelet	44
Figure 4-14: Healthy Location Coefficient plot with Scale Value 1 using Haar Wavelet	44
Figure 4-15: DWT Filtering	46
Figure 4-16: DWT Co-efficient	46
Figure 4-17: DWT Level 1 Coefficient Healthy	47
Figure 4-18: Complete DWT Result	47
Figure 4-19: SWT Coefficient at Cracked Location	48
Figure 4-20: Healthy Location SWT Coefficient	48
Figure 5-1: Flow Graph for Hilbert Huang Transform Process	51
Figure 5-2 : Signal with marking of Upper Envelop (blue) and Lower Envelop (Red)	52
Figure 5-3 : Mean Value Calculation. Curve mentioned in Pink is plot of mean values	52
Figure 5-4 : Residue Plot, obtained after subtracting mean value from original signal	53
Figure 5-5 : IMF plots using EMD Process	54
Figure 5-6: Hilbert Huang Spectrum	55
Figure 5-7: Test Specimen with three machined cracks with Top View, Front view and Side View	56
Figure 5-8: A-Scans Plot of Healthy and Cracked Location. (a) Healthy Location. (b) Cracked Location having Crack of 3-mm. (c) Cracked Location having Crack of 4-mm. (d) Cracked Location having crack of 5-mm	57
Figure 5-9: Healthy Location IMFs	58
Figure 5-10: Cracked Location IMFs, Crack of 5-mm dia. at depth of 8-mm	58
Figure 5-11: Hilbert Spectrum. (a) Healthy Location. (b) Cracked Location, crack of 3-mm dia. (c) Cracked Location, crack of 4-mm dia. (d) Cracked Location, Crack of 4-mm dia.	59
Figure 5-12 : ROI HHT Spectrum of each Location. (a) Healthy Location. (b) Cracked Location, crack of 3-mm dia. (c) Cracked Location, crack of 4-mm dia. (d) Cracked Location, Crack of 4-mm dia.	60

List of Tables

Table 2-1: Aerospace Material Test Issues	17
Table 3-1: Calibration Standard used for Aerospace NDT using UT	24
Table 5-1: Crack Dia. Dimensions.....	56
Table 5-2: Energy Distribution between 6 mm till 10 mm depth of Specimen	61

LIST OF ABBREVIATION

NDT	Non Destructive Testing
UT	Ultrasonic Testing
FFT	Fast Fourier Transform
STFT	Short Term Fourier Transform
WT	Wavelet Transform
CWT	Continuous Wavelet Transform
DWT	Discrete Wavelet Transform
SWT	Stationary Wavelet Transform
HHT	Hilbert Huang Transform
EMD	Empirical Mode Decomposition
HS	Hilbert Spectrum
SDMS	Sonatest Data Management Software

CHAPTER 1

1 INTRODUCTION

Aircraft structures are subject to various types of loading conditions, mainly during take-off, landing, and maneuverings. Such operating conditions can lead to the development of fatigue cracks in the aircraft structure. Due to the stress concentration fatigue cracks often initiate at the fasteners connecting multiple metallic layers. Because of their ability to propagate over long distances, ultrasonic NDT offer an efficient way for the Non-Destructive Evaluation (NDE) and Structural Health Monitoring (SHM) of large areas. Nondestructive testing plays a significant role in manufacturing, quality control and structural health monitoring to ensure safety and reliability. Ultrasonic testing (UT) is one of the most widely used NDT methods, and has many applications in practical life. It has extensively been used in weld inspection [1], pipeline damage identification [2], characteristics of steel billets [3], inspection of nuclear power plant, Bridges and huge concrete structures [4], material characterization and identification [5], railway tracks inspection, aerospace structures' inspection[6]. UT has also been broadly used in medical applications. It is also a preferred choice for sub surface or internal surface cracks which are normally not seen through visual inspections. In ultrasonic testing, high frequency sound waves are introduced in the component / sample under inspection and their reflections are received / processed for analysis. Ultrasonic waves are reflected back due to the change in acoustic impedance within the sample. The acoustic impedance change is due to discontinuities, or presence of voids /cracks, which are detected and analyzed.

Ultrasonic testing is the most suitable technique for inspecting planar discontinuities lying parallel to the test surface. Ultrasonic testing also offers an edge while inspecting aircraft structures as only one side of the test area needs to be accessible. Crack sizing, Crack detection, thickness measurement, inclusions and porosity detection, inspection of honey comb structures are some of the inspections offered by ultrasonic testing while inspecting aerospace structures [6].

The topic of the MS thesis is a preliminary study of the application of ultrasonic testing for the monitoring of crack in an aircraft structures using modern signal processing algorithms

1.1 Motivation

Assuring aircraft safety, while controlling operating costs, is one of the capital objectives for aircraft companies. A report from AIRBUS [7] stresses this fact, saying that operating costs such as fuel have little potential for further diminution, while the maintenance costs can be further diminished in the future. Maintenance costs could also become a major concern for airlines with ripening aircraft fleet, as the workforce required for inspection is increasing with the aircraft's life. Numbers given by Sampath indicate that the man-hours required for inspecting and repairing the damage of an EF-111A fighter increased by 400% during ten years [8]. Holes for fasteners and rivets connecting multiple metallic layers in aircraft structure are some of the locations where damage like fatigue cracking often appears due to the stress compactness. The result of a major airframe fatigue test performed on a Tornado fighter aircraft showed that 70% of the damage on this aircraft resulted from fatigue cracking in the different structural layers, occurring mostly at fastener holes, joints, rivets and bolts [9]. Some of the current inspection techniques used for aircraft maintenance involve time consuming and intricate procedures. This

can make such techniques very labor intensive and overpriced. Many aircraft structures require removal of multiple structural components to detect flaws in the internal layers of the structure [10] by visual inspection. This procedure for the inspection of multi-layered aircraft structure is fairly ungainly, resulting in significant down time for aircrafts.

Studies by the aircraft industry have demonstrated that an aircraft SHM system could result in considerable maintenance cost and downtime diminution [11, 12]. On the grounds MS thesis investigates the sensitivity of ultrasonic waves to detect such defects, as it could be used in SHM of aircraft structures.

1.2 Objective

Following objective are intended to be achieved

1. Independence from OEM set up
2. Insight and better comprehension of NDT signals would help in accessing the integrity and validation of repair activities
3. If a component failure is incorrectly diagnosed one or many times, that clearly represents an increased requirement for maintenance human resources as well as facilities. A related factor that often is not considered is the wear that occurs as a result of multiple repair attempts. Not only are components damaged as a result of un-necessarily replacement but additional wear and costs are incurred
4. Safety of the aero plane enhances through ensuring structural integrity
5. A great financial advantage due to reduction in down time of aero planes by timely planning of repair/replacement action.
6. The proposed method will improve aircraft reliability and availability through intelligent mission as well as maintenance (repair/replacement) planning and scheduling

1.3 Outline of the Thesis

This thesis report is organized as follows

Chapter 1: Introduces the motivation of the thesis following core objective of the research work
.It further outline the contents of next chapters

Chapter 2: Provides a brief literature review of non-destructive testing, background and physics of ultrasonic testing and its application in aerospace industry

Chapter 3: Describes the experimental setup for NDT, software used and calibration procedure for UT NDT. Choice of calibration standard is also discussed in this chapter followed by time domain analysis on acquired ultrasonic non-destructive testing signals. Data format analysis and standard data presentation formats are also briefly described in this chapter

Chapter 4: Describes FFT, its application on ultrasonic signals followed by results and shortcomings of FFT and its remedy using Short Term Fourier Transform. Mathematical description of STFT and results of STFT are discussed in this chapter. It also covers the short details about theory, and application of Wavelet transform. Continuous wavelet Transform (CWT), Discrete Wavelet Transform (DWT) and Stationary Wavelet Transform are covered here

Chapter 5: Flaw characterization using Hilbert Huang Transform is described in this chapter
.Further it evaluates the results based on proposed HHT method

Chapter 6: It concludes the thesis and provides possible direction for Future Work

CHAPTER 2

2 ULTRASONIC NON DESTRUCTIVE TESTING

2.1 Introduction to Ultrasonic Non-Destructive Testing

Ultrasonic Testing (UT) uses high frequency sound energy to conduct examinations and make measurements. Ultrasonic inspection can be used for flaw detection/evaluation, dimensional measurements, material characterization, and more.

2.2 History of Ultrasonic

Precedent to World War II, sonar, the technique of sending sound waves through water and perceiving the returning echoes to characterize submerged objects, inspired early ultrasound scrutinizers to explore ways to apply the concept to medical diagnosis. In 1929 and 1935, Sokolov explored the use of ultrasonic waves in detecting metal objects. Mulhauser, in 1931, acquired a permit for using ultrasonic waves, using two transducers to apprehend flaws in solids. Firestone (1940) and Simons (1945) developed pulsed ultrasonic testing using a pulse-echo technique.

Shortly after the end of World War II, researchers in Japan began to scrutinize the medical diagnostic competence of ultrasound. The first ultrasonic instruments were presented with blips on an oscilloscope screen used in an A-mode. That was followed by a B-mode presentation with a two dimensional, gray scale image.

Until 1950s, Japan's work in ultrasound was relatively unknown in the United States and Europe. Scrutinizers then presented their findings on the use of ultrasound to perceive gallstones, breast masses, and tumors to the international medical community. Japan was also the first

country to apply Doppler ultrasound, an application of ultrasound that detects internal moving objects such as blood coursing through the heart for cardiovascular investigation.

Ultrasound founding fathers working in the United States contributed many revolutions and important discoveries to the field during the following decades. Sucrutinizers learned to use ultrasound to perceive potential cancer and to visualize tumors in living subjects and in excised tissue. Real-time imaging, another significant diagnostic tool for physicians, presented ultrasound images directly on the system's CRT screen at the time of scanning. The invention of spectral Doppler, and later color Doppler illustrated blood flow in various colors to stipulate the speed and direction of the flow.

The United States also introduced the earliest hand held "contact" scanner for clinical use, the second generation of B-mode equipment, and the prototype for the first articulated-arm hand held scanner, with 2-D images.

2.3 Advantages of UT

Ultrasonic Inspection is a very useful and versatile NDT method. Few advantages of ultrasonic testing that are often referred include:

- It is sensitive to both subsurface and surface discontinuities and cracks.
- The depth of penetration of ultrasonic for flaw detection or measurement is better to other NDT methods.
- With the help of pulse echo technique only single sided access of test part is needed.
- It is highly accurate in determining reflector position and estimating size and shape.
- Minimal part preparation is required.
- Instantaneous results can be obtained using electronic equipment.

- Automated system can be used for production of detailed images
- It can also be used for thickness measurement

2.4 Disadvantages of UT

As with all NDT methods, ultrasonic inspection also has its limitations, which include:

- Surface must be reachable to conduct ultrasonic testing.
- More Skill and training is required as compared to other methods.
- Use of coupling medium is essential to promote the transfer of sound energy into the test material
- Materials that are irregular in shape, rough, very small, exceptionally thin or non-homogeneous are difficult to inspect.
- Cast iron and other coarse grained materials are difficult to inspect due to low sound transmission and high signal noise.
- Linear defects oriented parallel to the sound beam may go undetected.
- Equipment calibration and the characterization of flaws needs reference calibration standard.

2.5 Aerospace Application of Ultrasonic Testing

Ultrasonic plays a critical role in the production and in service testing of aerospace structures. It is applied to metallic and composite parts using a wide range of techniques, frequencies and waveform types. The applications can be routine or unique. The ultrasonic testing checks for discontinuities such as cracks, delamination, porosity and inclusions. Ultrasonic may also may also be used to measure dimension and material properties. Table 2-1 lists aerospace materials that are ultrasonically tested. For

the most parts ultrasound is best when inspecting for planar discontinuities laying parallel to the test surface. If the back surface of object is also parallel it simplifies the test.

Cracks are developed on aircraft structures due to stresses experienced during flight and landing. Composite structures are subject to impact damage from birds, hail service vehicle and other sources. Numerous location on aircraft are made up of multiple layers of detail components joined together by rivets or bolts fastener. At these locations, it is possible for cracks to be generated in subsurface member and go undetected until they propagate to a surface. Early detection of subsurface crack is possible with ultrasonic testing. Composite assessment on aircraft structures is based on visual inspection followed by ultrasonic testing. [6]

Table 2-1: Aerospace Material Test Issues

Material	Inspection Issues	Ultrasonic Testing
Honey Comb Core Structure	Bonding of Core to Skin, Damaged Core , Filled Core , Inclusions	Through-Transmission Technique is Common
Carbon to Carbon	Dry Ply, Porosity , delamination , wrinkles	Ultrasonic Testing detects delamination and Porosity
Castings	Cracking, Voids/ Porosity , Weld Repairs , Dimensional Tolerances	Pulse Echo Angle beam , normal beams and phased array are used to detect and locate discontinuities
Machined Parts	Cracks , Residual Stress , Dimensional Tolerances , Repairs	Pulse Echo Angle beam and phased array are used to detect and locate discontinuities
Fastened Structure	Cracks, Corrosion	Pulse Echo Angle beam and phased array is used to detect cracks around fasteners. Normal beam Ultrasonic Testing is used for corrosion detection
In-service or Damage Structure	Impact Damage , Heat Damage , Fatigue Cracks , Corrosion , Disbonds and Delamination	Ultrasonic Testing is useful for composite impact damage, disbonds and delamination with normal beams. Moisture Ingress can be detected through changes in wave speed and attenuation. Fatigue crack in top layers are detectable with normal and angle beams. Thickness Changes in accessible layer indicate corrosion

3 EXPERIMENTAL SETUP AND TIME DOMAIN ANALYSIS

3.1 Ultrasonic NDT Setup

A typical UT inspection system consists of several functional units, such as the pulser/receiver, transducer, and display devices. A pulser/receiver is an electronic device that can produce high voltage electrical pulses. Driven by the pulser, the transducer generates high frequency ultrasonic energy. The sound energy is introduced and propagates through the materials in the form of waves. When there is a discontinuity (such as a crack) in the wave path, part of the energy will be reflected back from the flaw surface. The reflected wave signal is transformed into an electrical signal by the transducer and is displayed on a screen. Figure 3-1 shows the reflected signal strength is displayed versus the time from signal generation to when an echo was received. Signal travel time can be directly related to the distance that the signal traveled. From the signal, information about the reflector location, size, orientation and other features can sometimes be extracted.

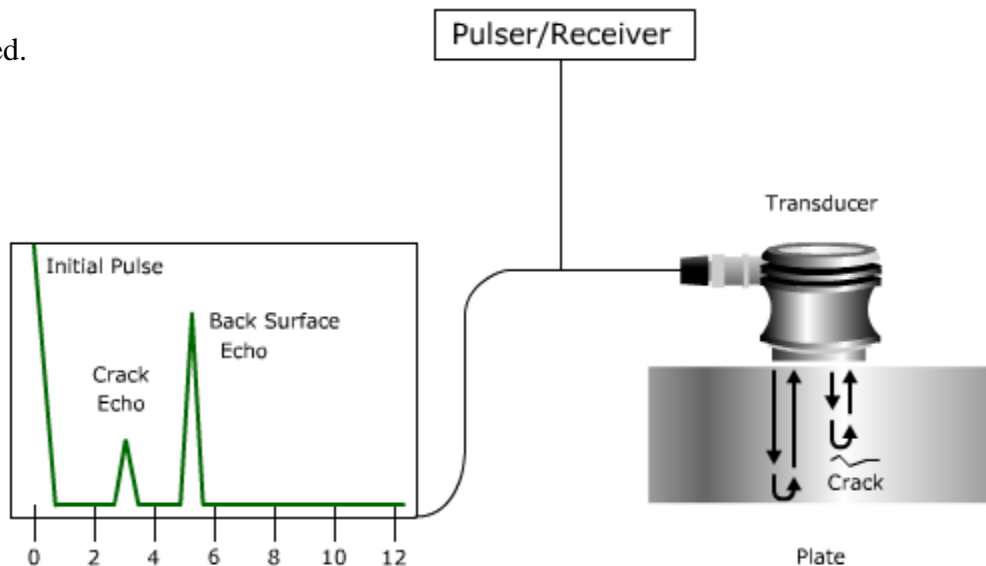


Figure 3-1: Basic UT-NDT Setup

3.2 Interface of Ultrasonic Equipment and Data Format Analysis

Development of algorithms using ultrasonic testing data of the aircraft first it was required to interface Ultrasonic Testing Equipment with our terminal so that we may process actual aircraft data at our PC or laptop and develop algorithms using engineering software's like MATLAB.

At PIA NDT Lab equipment from different vendors are available for data reading and forwarding that manual recorded data to OEM. Ultrasonic Testing equipment of GE, Sonatest and Olympus are mostly in use, we have interfaced below mention equipment.

- Master Scan 350M (Sonatest)
- USN 60 (General Electric)

Master Scan 350 M is successfully interfaced with our Desktop and as well as Laptop .We have successfully extracted and read the data format for further analysis. Sonatest Data Management Software is used to extract the data from equipment using serial port of the terminal, Figure 3-2 shows the SDMS screen and acquiring of data.

Acquired Data can be saved in three formats: those are .dat type file, .csv file and .dfd type format. .dat type format for algorithms development is used. In the data file there are 5 header lines and 255 data values.

Since to make it more convenient, we have interfaced Sonatest equipment with Windows 7 based system using USB port. Serial to USB cable has been used in order to make things more portable. Laptop with the equipment can easily be used in the field in order to get more results..

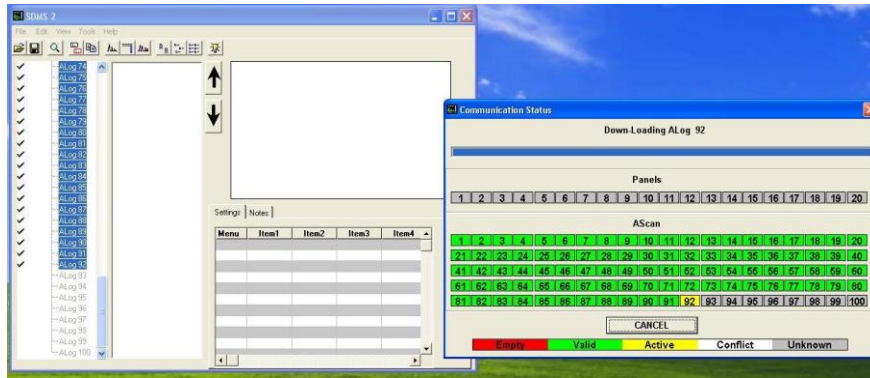


Figure 3-2: Acquiring Data Using Sonatest Data Management Software

3.3 Calibration Procedure

Before performing data acquisition on equipment it is essential to check the calibration. Calibration means standardization of the crack/flaw with respect to calibration block available as per recommendation by the manufacturer of the Aircraft, this needs to do before every measurement / reading or test in order to properly estimate the behavior of ultrasound on different type of crack.

Further there is one more calibration needs to be done, which is to make equipment calibrated. Manufacturer of the equipment recommend equipment calibration once in a year. Airline have to pay the charges of this calibration along with shipment charges both sides but there is still a chance of calibration lose during shipment so there are few organization in Pakistan which does this calibration like PCSIR.

Calibrated equipment was used for testing due to authenticity of the results. Aircraft manufacturer had already developed the procedure for flaw calibration and PIA NDT Team uses there recommended calibration standards to inspect the part of the aero-plane.

During Ultrasonic Testing inspection calibration was performed on calibration blocks made of same material as that of the aircraft component under test structure. Calibration procedure is as follow for the crack / flaw

- Set screen display so that it's range should be of same size as that of the test specimen
- Since ultrasound speed is different in different materials so it is required to set the sound speed as per pre-defined speed for that material
- Ultrasonic transducers works on different frequency when an electric pulse is applied. It is necessary to select the proper frequency value on equipment based on transducer
- Angle of the ultrasonic transducer also matters while carrying out the inspection. In order to get maximum reflections from the effected surface and to obtain benefit of the directed nature of the ultrasound angle is required to set.
- Probe delay is also the factor needs to set on equipment as per manufacturers advice
- Display Delay is also adjusted as per requirement by looking at the initial pulse
- Gates are used to monitor the pulse between defined parameters as per our requirement. Gates helps to neglect or select a pulse with different amplitude
- Last parameter that needs to adjust is Gain in db. Gain can be adjusted in order to get amplitude magnified and meaningful for our reading or inspection

After adjustment of above mention parameters, testing can be performed for one component/part of the aircraft. Values may vary while performing testing on same part of different type of airplanes.



Figure 3-3: Calibration Block for Thickness Calculation



Figure 3-4: Calibration block for testing at spindle

3.4 Choice of Calibration Standards

Calibration standards are the reference blocks used extensively in the field of Non Destructive Testing. These standards are provided by the aircraft manufacturer to the relevant Non Destructive Testing section of the airline if they are performing NDT. Figure 3-3 and Figure 3-4 shows the calibration blocks. These blocks are available for different parts of the aircraft, reference blocks are made of the same material as that of the aircraft component. These blocks are often embedded with artificial or self-created well dimensional cracks / flaws in order to estimate and detect the crack properly. Reference blocks are of different shape and size developed by the manufacturer, there is a serial number mentioned against each block which helps to work with that block. This serial number is very helpful for record keeping of NDT. OEM provides the Non Destructive Testing manual to inspect the concerned part, this manual is comprises of the procedure and steps that NDT Team needs to perform for evaluation of the crack. In aircraft industry NDT manual is called as NTM used for non-destructive inspection.

Choice of calibration standard is much more important. It is required to check for different parameters before performing NDT of the affected / diagnosed area. Few of them are mentioned below

1. Choice of Calibration Standard depends on the component or a part being inspected as we have to select the block of same area / component being inspected as we have selected Fuselage , Landing Gear and Wings Area for our research
2. Techniques that can be used on calibration block as in our case we have to only consider the reference blocks on which Ultrasonic Testing techniques can be performed
3. Checking for the equipment as if either it is available or not, in most of the cases for Ultrasonic testing PIA NDT team is using USN 60 and MasterScan Sonatest 350 M (which is also used in data acquisition for this research).
4. For ultrasonic testing on chosen calibration block, available frequency transducers selection is also important

Selection of calibration block needs proper reading of the material and manual as this selection helps to properly diagnose the affected area. Calibration blocks for different aircraft are different i.e. calibration for Boeing 737 on the reference block given by manufacturer cannot be used for same part of Air Bus 310

Table 3-1 shows the few reference standards or calibration blocks details which are finalized to be used in this project

Table 3-1: Calibration Standard used for Aerospace NDT using UT

S. No	Part of the Aircraft	ULTRASONIC TESTING	
		AIRBUS 310	Reference Block Serial No.
1	Fuselage	Fuselage internal structure	PN 99F53303020000
2	Landing Gear	Nose landing gear door actuator upper support attachment fitting.	PN 99A53003005001
3	Wings	Integrated stringers positions	PN 99A53307267000



Figure 3-6: Different Calibration Blocks



Figure 3-5: Ultrasonic Testing Transducers

3.5 Data Presentation

In order to present ultrasonic data in analyzable format first of all data was presented in three standard formats of ultrasonic non-destructive testing data. Three standard formats details are stated below along with the obtained results

1. A-Scan
2. B-Scan
3. C-Scan

3.5.1 A-Scan (Amplitude Scan)

A-Scan is the most common data presentation format of ultrasonic testing NDT technique. It is an acronym for Amplitude Scan means it displays the amplitude on Y-Axis and time or distance on X-Axis. Either time or distance is known, other value can be calculated based on simple distance formula as velocity of ultrasound in a specific material is constant.

$S=v*t$ can be used to calculate time or distance depends on the obtained data from the equipment. In MasterScan 350 M distance was presented on X-Axis so the format kept same for the acquired data. In A-Scan there are pulses at different locations. In case of any discontinuity, crack or any change of medium there is reflection which can be observed on equipment screen and saved in equipment for further data acquisition at laptop or PC. **Figure 3-7** shows the test piece which is used to perform ultrasonic testing



Figure 3-7 : Test Specimen used for Ultrasonic Testing

Test Block was marked with 25 data points having dimensions of 1 inch by 1 inch due to diameter of transducer. A total of twenty five values were obtained with the help of ultrasonic transducer and equipment. Those values were first acquired from the equipment using Sonatest Data Management Software (SDMS) and further analyzed in MATLAB

Figure 3-8 shows the 25 A-Scans of the test piece which is showing three pulses in almost every test location

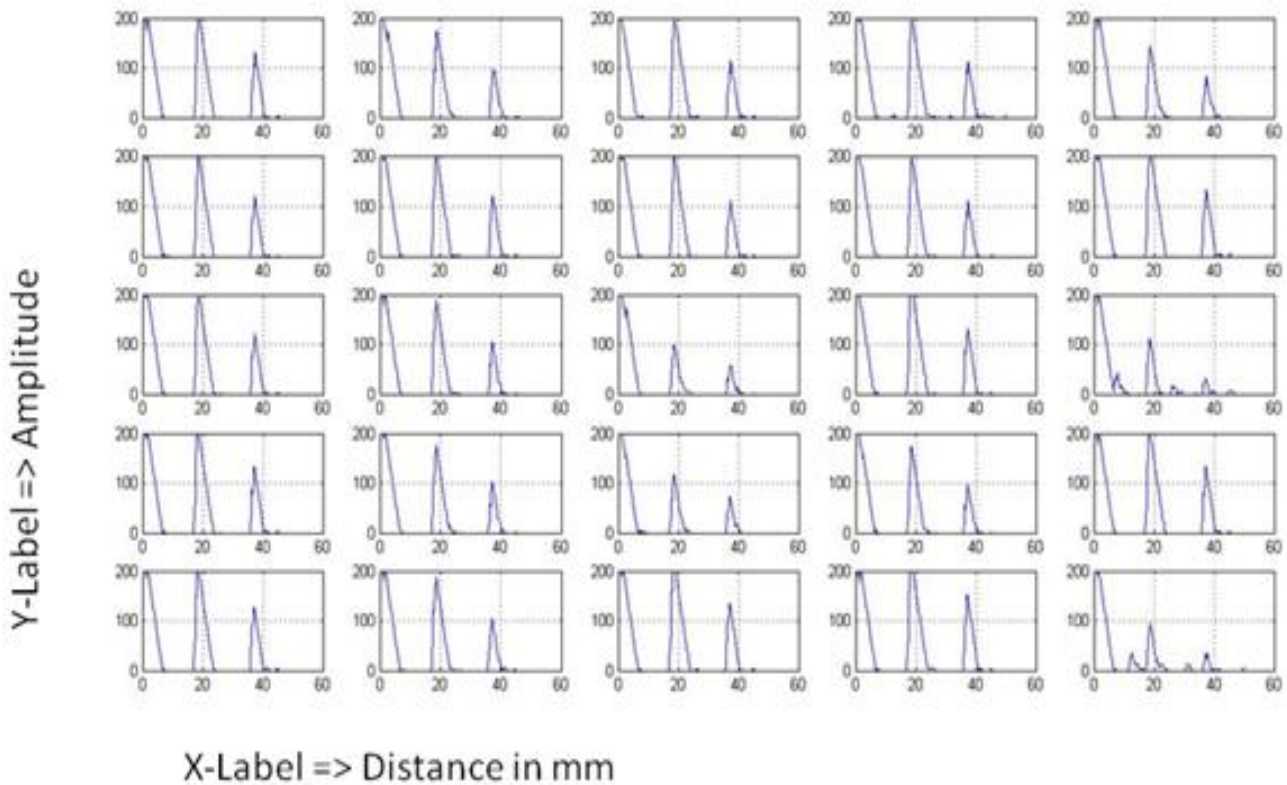


Figure 3-8: A-Scan plots of 25 Locations of the Test Specimen

First pulse is initial pulse, dead zone would be more appropriate as even without placing transducer on test piece 1st pulse arises , second pulse is back wall reflection or back surface reflection which arises at near about 19 mm which is the approximate thickness of selected test specimen . Third one is the repetition of the back wall reflection pulse. It is evident from plots of Figure 3-8: A-Scan plots of 25 Locations of the Test Specimen that we have some discontinuity, crack

or any flaw at location 15 and at location 25. Test piece has two holes at stated locations i.e. at location 15 and at location 25 now these two locations would be focused to analyze further in order to estimate the actual size of crack or flaw characterization

Figure 3-9 shows the single A-Scan with initial pulse and back surface reflection

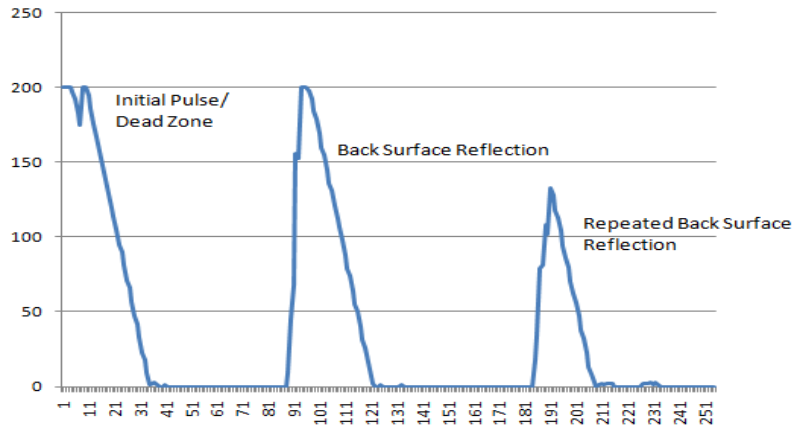


Figure 3-9: Sample A-Scan, with initial pulse and back surface reflection marking

3.5.2 B-Scan (Cross Sectional View)

B-Scan is cross sectional view of the test specimen displayed graphically. B-Scans also termed as brightness scan is obtained with the help for A-Scans at predetermined intervals. This is 2-D type of plot in which we have linear distance on which scans are obtained displayed at X-Axis, Y-Axis shows the depth of the test material and color shows the intensity of the pulse at specific location.

B-Scan, here, is obtained by taking five cross sections of the test piece. Those are plotted accordingly to get the better understanding of the exact location of the crack. Cross Section of the first slice of the test specimen is mentioned in Figure 3-10

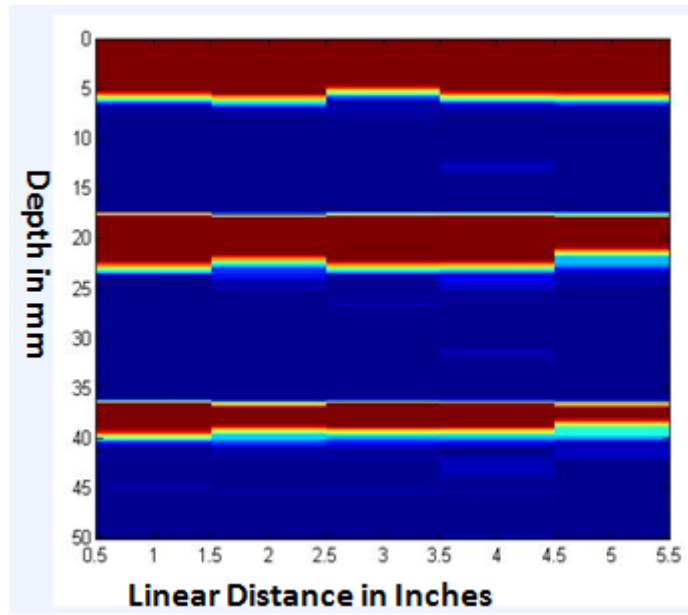


Figure 3-10: B-Scan or Cross Sectional View of Test Specimen

3.5.3 C-Scan (Top View)

C-Scan is top view of the test area and it can further be said that it is top view thickness mapping of the material which is obtained with the help of A-Scans. Thickness is calculated with the help of amplitude scans and plotted accordingly. In C-Scan view we have dimensions (Length and Breadth) of the actual piece on X-axis and Y-Axis and their thickness is along the Z-axis. With the help of C-Scan we can estimate the sub surface issues without wearing and tearing. Below mention Figure 3-11 shows the C-Scan of the test specimen

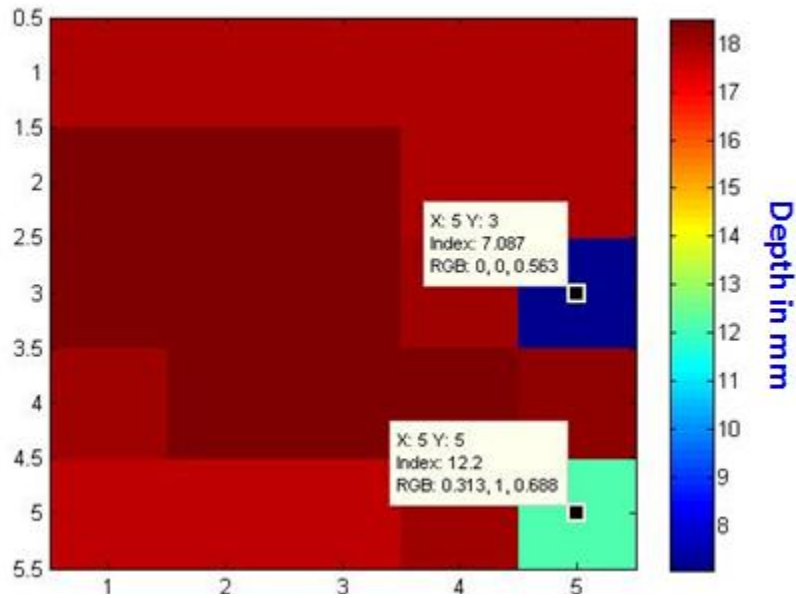


Figure 3-11 : C-Scan View of the Test Specimen

3.6 Time Domain Analysis Short Comings

A-Scan, B-Scan and C-Scan data presentation is time domain representation of the ultrasonic testing signals. Time domain obtained results are not sufficient for flaw characterization and exact crack localization. From the above different plots it can be assumed that crack is too large and have dimensions of 1 by 1 inches at particular location further crack is regular with square shape. Whereas this is not true crack size is of 5 mm in depth and at location of approx. 7.2 mm depth and one is at 12 mm depth. Cracks are circular drills having diameter of not more than 7-8 mm. It is also not clear that either the acquired pulse is from crack or because of some type of noise

In order to get more precise behavior of the crack it was concluded to shift to frequency domain analysis so that the hidden features can be obtained. Frequency domain analysis is also become necessary due to non-periodic behavior of the ultrasonic NDT signal. Behavior of signals, from different types of problems on aircraft structure also leads towards frequency domain analysis.

4 FREQUENCY AND TIME FREQUENCY ANALYSIS

4.1 Introduction

Transforms are used to analysis signal in frequency domain. Frequency domain representation and analysis gives insight look of the time domain or raw signal resulting in some meaning full conclusion. Time domain signals are also termed as raw signals due to very less information about the acquired signal being observed. Further it is not an easy task to get information about abrupt changes and small discontinuity when considering distance-amplitude signals. Ultrasonic signals are reflections from the discontinuity or change of medium or more precisely when there is any acoustic impedance mismatching it caused ultrasonic pulse.

4.2 Fourier Transform

Fourier transform is one of the basic techniques used for signal characterization in frequency domain. In this method multiplication is performed with the signal under observation and with sine and cosine functions. With the help of some plotting tools in MATLAB and basic understanding regarding Fourier analysis below mention plots are obtained by selecting 20-MHz as sampling frequency. Sampling frequency is selected based on Shannon Frequency Theorem as transducer used to carry out examination was of 5-MHz frequency

While looking at the plots of the signal obtained at the location of crack it has been observed that changes occur in low frequency components of the signal with respect to 5-MHz transducer generated frequency. Figure 4-2 and Figure 4-3 shows that there is visible effect on lower side

lobes of the Fourier transform plot which indicates that frequency modes are changing whenever there is any crack.

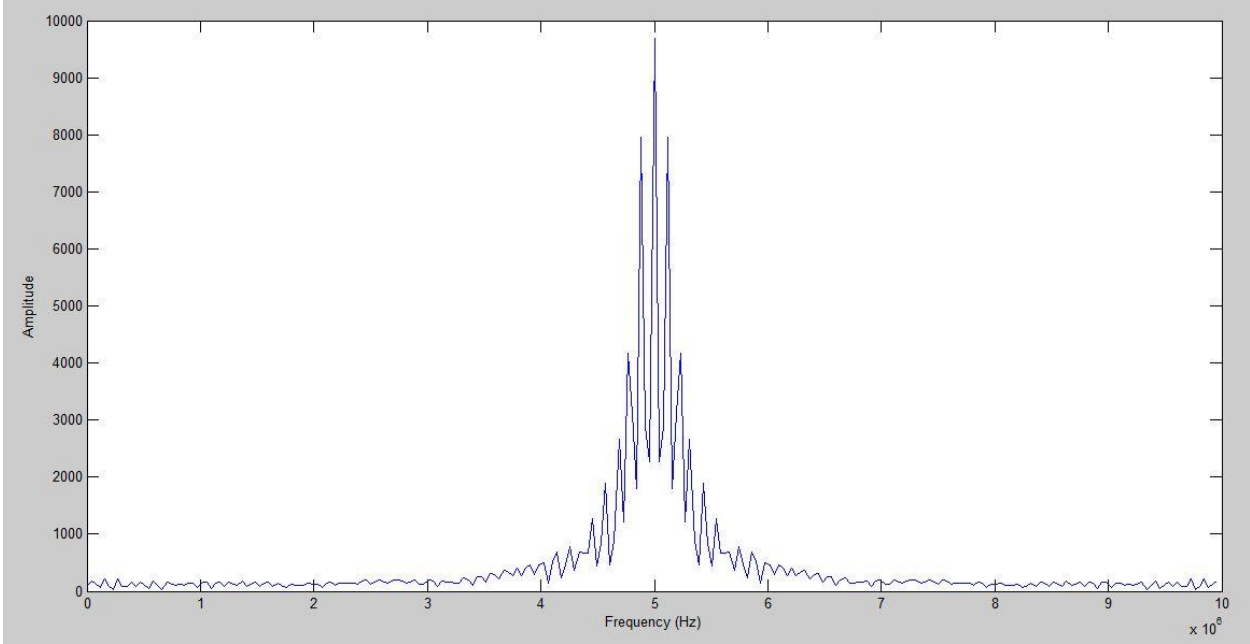


Figure 4-1: FFT at Healthy Location

Fourier transform plot for location 1 with the help of 20-MHz sampling frequency

Fourier Transform plot for location 15 i.e. at crack location with 20-MHz Sampling Frequency

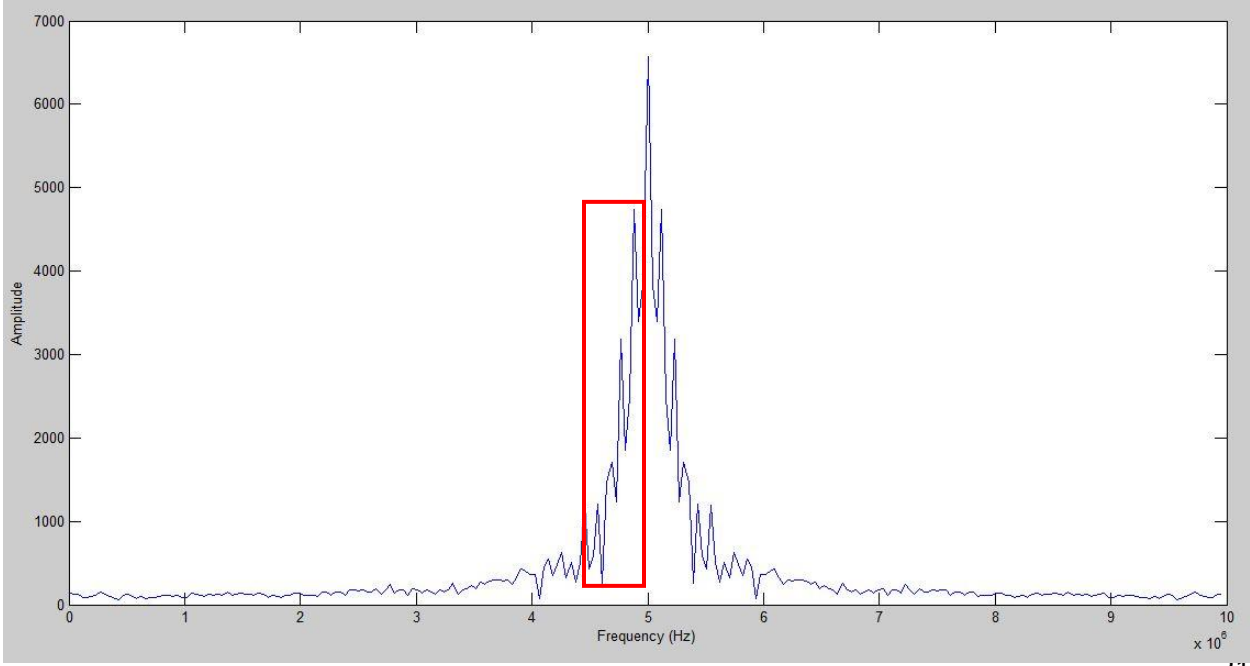


Figure 4-2: FFT Spectrum at Cracked Location

From the above two spectrums based on Fourier Transform techniques it is clear that there is prominent change in side lobes of the plot obtained at location with crack and without crack with center frequency is exactly at 5-MHz indication

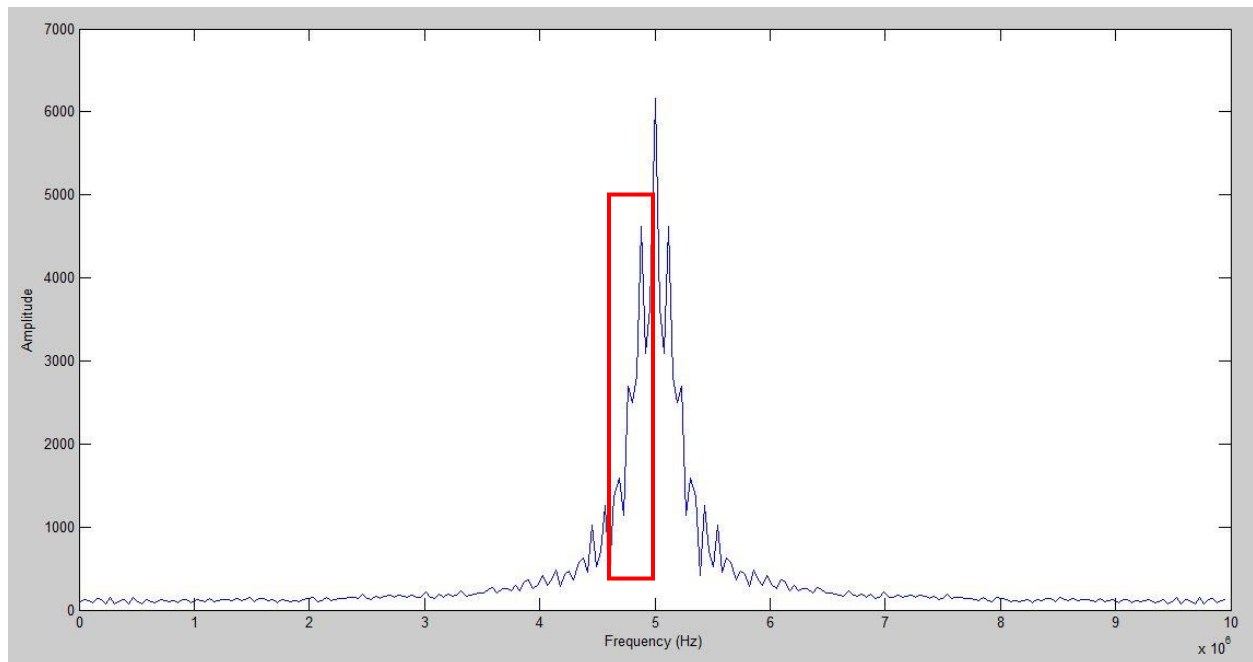


Figure 4-3: FFT Spectrum at Cracked Location

Same could be observed at location 25 which is another cracked location. There is no change in center frequency of the spectrum

4.2.1 Fourier Transform Based Classification and ROI Detection

Fourier transform is effectively utilized to obtain the features of time domain signals, obtained results gave little bit information. Results based on this technique are not useful for flaw characterization and ROI detection rather they are only giving information about that at what frequency signal is changing its behavior. Since basic aim was to get the time frequency information which is not fulfilled here so it is required to move to some technique which clearly specify the effects of frequency at particular time so that time information can further be transformed to get information about distance.

Currently it cannot be stated that any useful region of interest is determined and flaw could be classified along with particular location. In addition the signal obtained from Ultrasonic NDT technique is non-stationary in nature and Fourier is not suitable for this due to its global representation of signal in frequency domain. It only gives information about the effect on frequency whereas it is much needed to have information about effect on frequency based on time. In simple words time frequency localization will help to get more appropriate information about the crack based on signal processing algorithms.

Time-Frequency representation can further be formulated into distance-frequency representation by using simple distance time formula i.e. $\text{Distance} = \text{Velocity} * \text{Time}$, Ultrasonic velocity for particular medium or material is constant. By doing this exact location of crack can be determined and its effect on frequency can be characterized which is not possible only with Fourier transform technique as ultrasonic NDT signals are non-stationary signals i.e. there frequency changes with time.

4.3 Short Time Fourier Transform (STFT)

STFT also termed as windowed transform was developed to overcome the shortcomings of Fourier Transform. Windowed transform utilizes the same idea of multiplication and background of Fourier Transform whereas now a window is multiplied with the signal instead of sine and cosine. Window is of limited duration and it is also time shifted till the end of signal, means multiplied at each location. This window multiplication leads to a very good time-frequency representation of the actual time domain signal

Below mention is the equation for STFT

$$STFT_f^u(t', u) = \int_t [f(t) \cdot W(t - t')] \cdot e^{-j2\pi ut} dt$$

Where,

$STFT_f^u(t', u)$ = Time Frequency Representation

$f(t)$ = Time Domain Signal

$W(t - t')$ = Window Function centered at $(t - t')$

Selection of window is essential for using STFT technique. Window should be selected so that portion of signal became stationary. Any type of window i.e. triangular, rectangular, Hanning or any other type of window can be selected or even one can form his own window as per requirement. It is better to select such window whose shape is near about or same as compared to the original signal. By doing this one can get good features of the raw signal

Selection of window is also a tradeoff between time-frequency representations i.e. a very large size window will result in good frequency information but time information will be lost and same selection of narrow window will lost frequency information whereas time information will be good enough.

Result of STFT in three axes plot with time information in on X-Axis, Y-Axis represents frequency information and Z-Axis shows the amplitude of the signal. Figure 4-4 is the spectrum of location 1

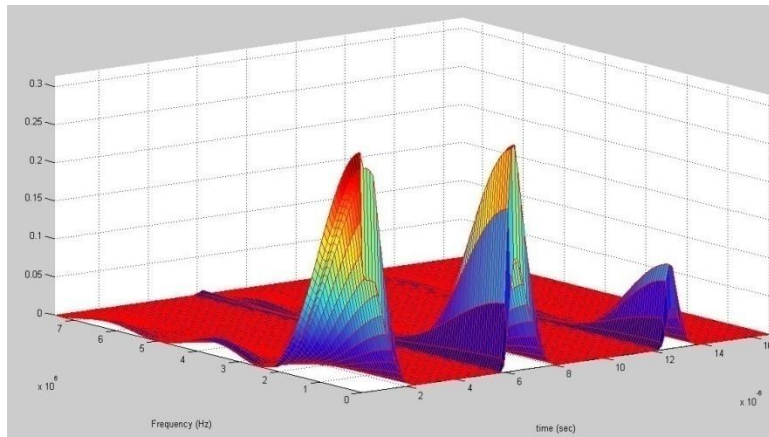


Figure 4-4: STFT Spectrogram of Healthy Location

STFT plot is obtained using 6 point rectangular window as it was required to get information about abrupt changes and discontinuity. A-Scan data on which STFT is applied is of 255 samples. Figure 4-5 is another STFT plot from location where we have crack i.e. at location 15

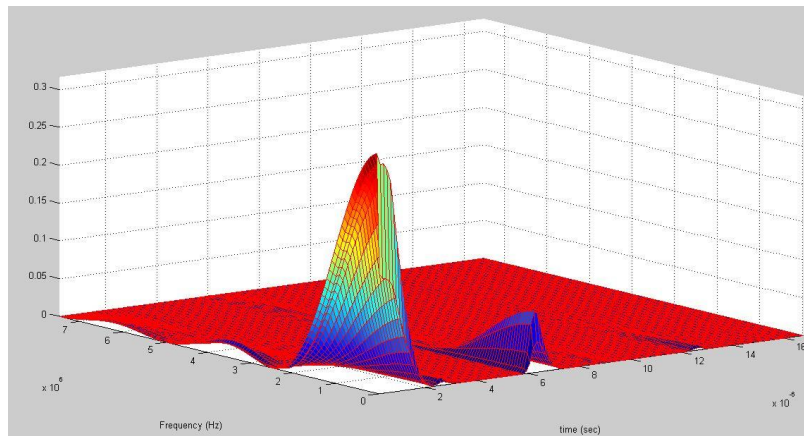


Figure 4-5: STFT Spectrogram Plot at Cracked Location

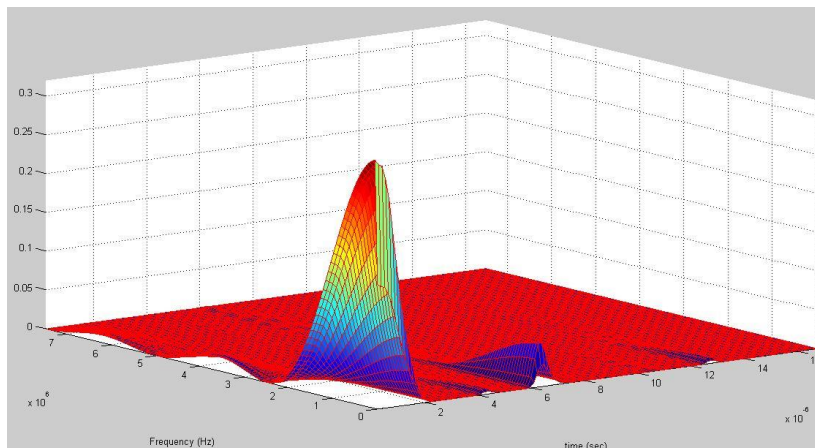


Figure 4-6: STFT spectrogram Plot at Cracked Location

From previous mentioned plots of Figure 4-4, Figure 4-5 and Figure 4-6 it is evident that at crack locations something is going to happen but in order to get more precise information from STFT plots five different locations are selected to check the time-frequency response of signal. Below mention are the effects of crack on pulse data at particular time with respect to frequency. Here time is further pointed as distance in order to get more accurate knowledge of crack / flaw. This will also help us for flaw characterization

Effects on frequency modes along with specific time (distance) localization is mentioned below

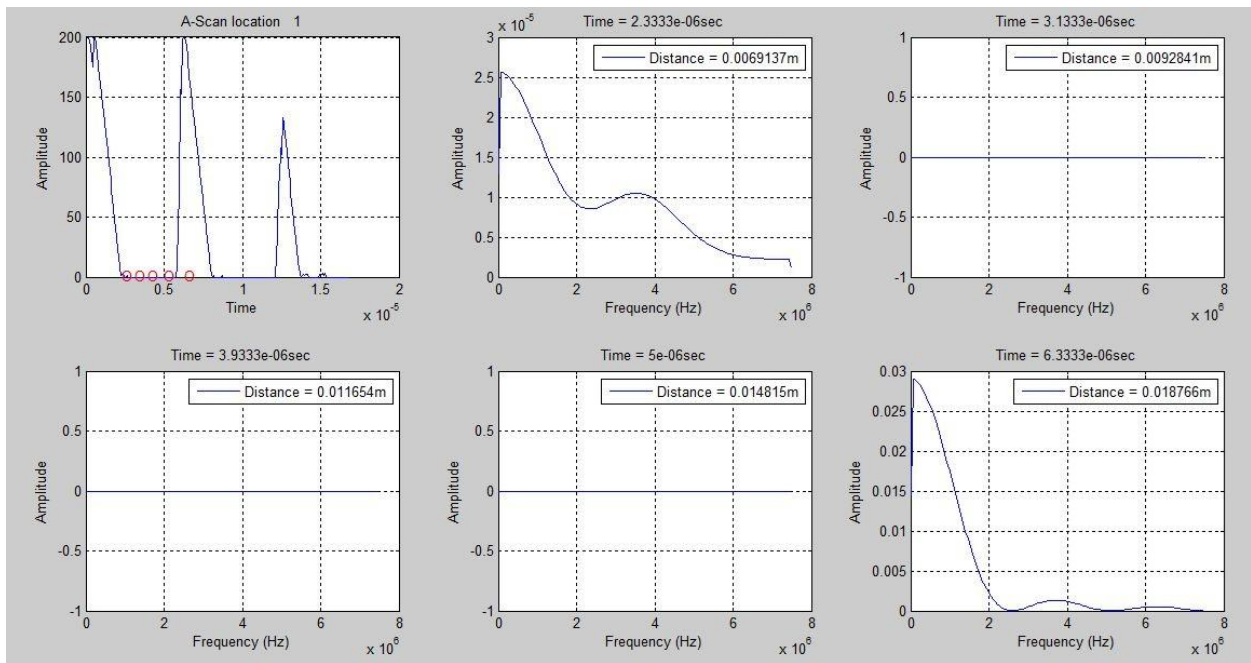


Figure 4-7: Healthy Location Frequency Plots at particular Distance

These plots are acquired from STFT spectrum plot at particular distance or at particular time. Remember that there was no crack at location number 1 of the test piece. Five points selected on each plot are as follows

1. At distance of 6.9 mm (till 6.5 mm we have initial pulse or dead zone) corresponds to time 2.33 μ sec

2. At distance of 9.28 mm corresponds to time 3.133 μ sec
3. At distance of 11.65 mm corresponds to time 3.93 μ sec
4. At distance of 14.81 mm corresponds to time 5 μ sec
5. At distance of 18.76 mm (this is near the back surface of the test piece) corresponds to time 6.33 μ sec

At location 15 of the test specimen we can see the clear effects on frequency component at that particular point

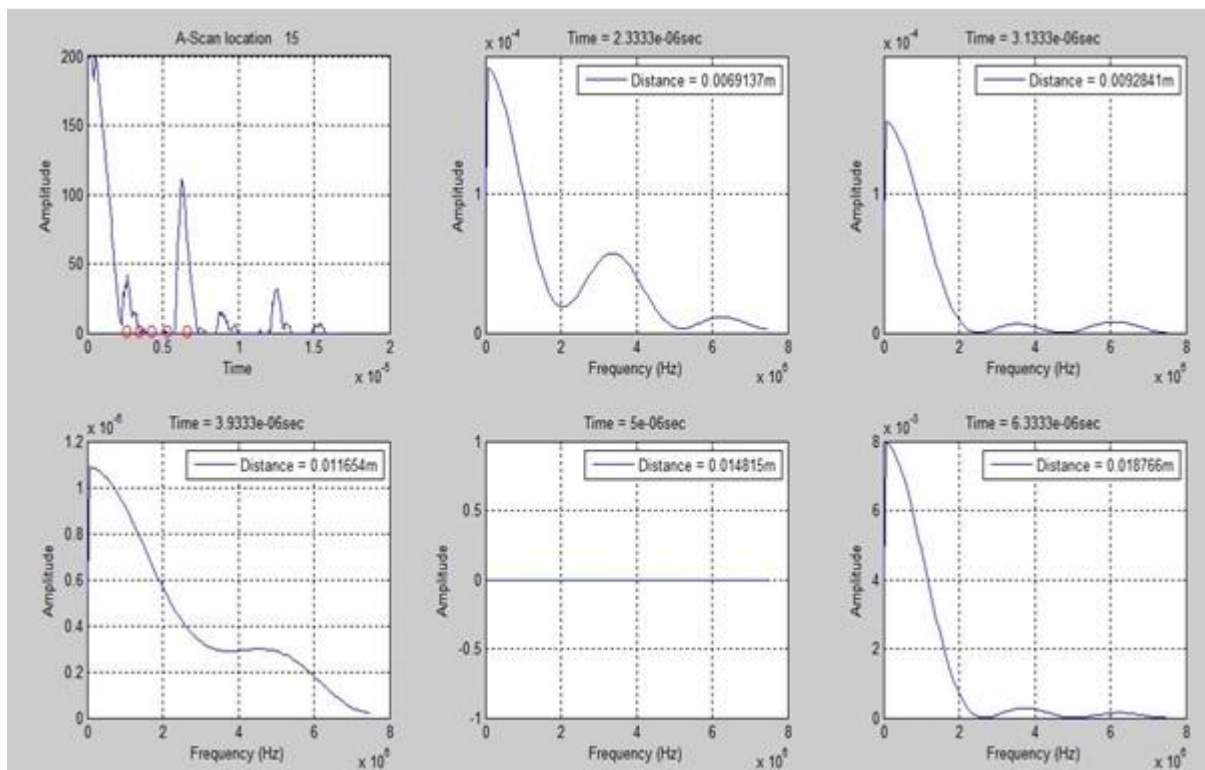


Figure 4-8: Cracked Location STFT Spectrogram Plot Threads

Same can be observed at location 25 plot as plotted in Figure 4-9

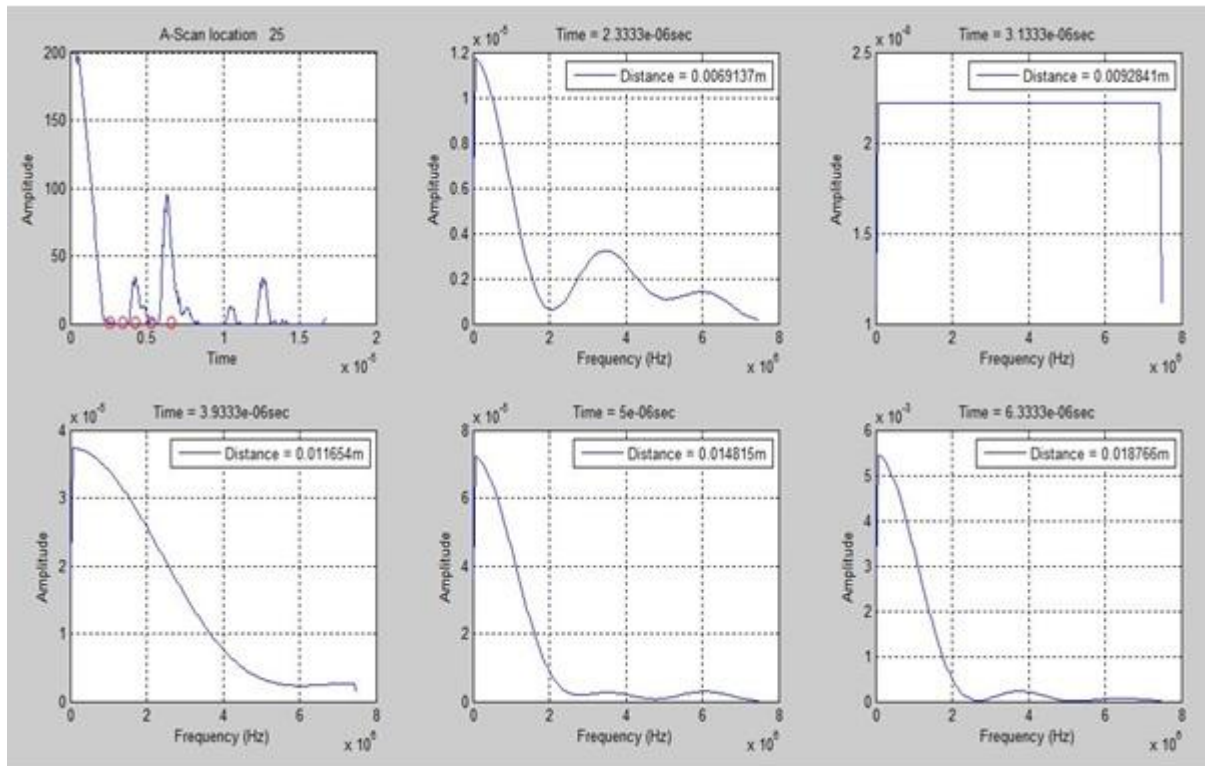


Figure 4-9: Cracked Location STFT Spectrogram Threads

As discussed earlier for STFT it is essential to keep window size same for the analysis of complete signal without considering the requirement of high and low frequency components. Window size leads to the multi resolution problem i.e. high size of window provides good frequency analysis and low size of window gives good time information but on the account of time and frequency information wastage respectively. It is also worth knowing that for practical signals high frequency remains in signal for short time whereas low frequency components remain there in the signal for significant duration. So in order to resolve this multi resolution problem an approach is used, to get good frequency resolution and poor time resolution at low frequency and good time resolution and poor frequency resolution at high frequency, named multi resolution analysis

Wavelet Transform was developed to overcome the shortcomings of STFT. In next section wavelet concept and the result obtained based on Wavelet Analysis along with different types of wavelet will be discussed

4.4 Wavelet Transform

There are three major types of wavelet transform which are as follows

1. Continuous Wavelet Transform (CWT)
2. Discrete Wavelet Transform (DWT)
3. Stationary Wavelet Transform (SWT)

4.4.1 Continuous Wavelet Transform (CWT)

Continuous Wavelet transform overcomes the resolution problem of STFT as discussed earlier. Major difference between STFT and CWT (continuous Wavelet Transform) is of variable size window. In CWT window is not fixed size as it was in STFT. Mathematical Equation of CWT is given below

$$CWT_x^\psi(\tau, s) = \frac{1}{\sqrt{|s|}} \int x(t) \cdot \psi^* \left(\frac{t - \tau}{s} \right) dt$$

In above mention equation the term $\psi^* \left(\frac{t - \tau}{s} \right)$ represents wavelet window generally and it is called as mother wavelet. Mother Wavelet is prototype for all other wavelets involved in computation. Mother wavelet is dependent upon two parameters ' τ ' and ' s ' i.e. translation and scale respectively. Concept of translation and scaling is discussed below

4.4.1.1 Translation

Translation is simply time shifting of a wavelet (small window) that is used for computation or calculation of correlation value between signal and wavelet

4.4.1.2 Scaling

Scaling in wavelet domain meant dilating or compressing the window by some factor. Scaling is reciprocal of frequency i.e. decreasing scale by factor 2, compresses the signal.

Scaling and translation (time shifting) is depicted in Figure 4-10

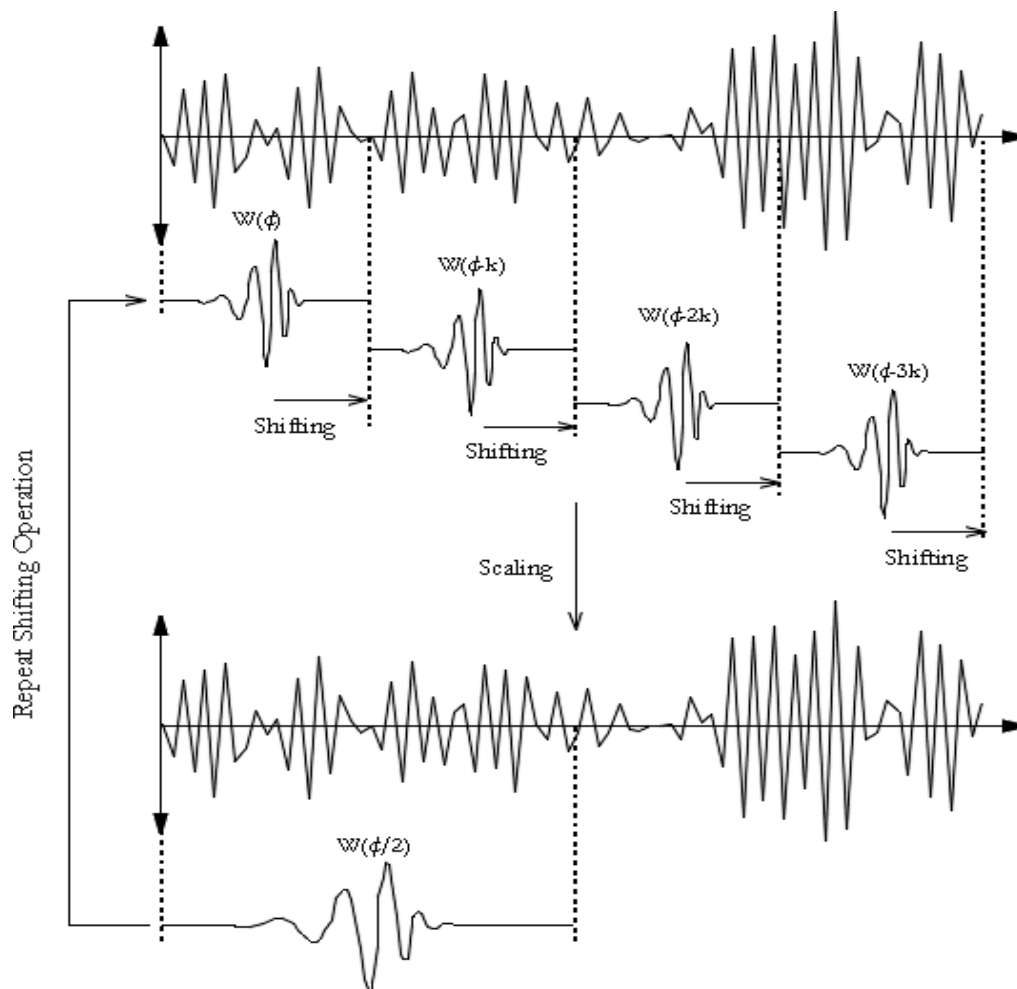


Figure 4-10: Scaling and Shifting Process using Mother Wavelet

Scaling and Translation makes CWT a tool to overcome the constant window problem of STFT. There are many pre-defined windows available those can be used with signal depending upon type of signal features required. Haar , Hanning , Hamming , Morlet and many other windows are available . One can drive his own window but it should be kept in mind that window have to satisfy below mention constraints

1. It should be of limited duration
2. Has an average/mean value of zero
3. Should have finite energy

4.4.2 Steps Involved in CWT Coefficients Calculation

One of the differences between Fourier Transform and CWT is the process of correlation coefficients calculation. In case of Fourier sine and cosine are multiplied and if there exists, a particular frequency component it gives visible or high peak at that point and for lesser similarity low peaks or no frequency component could be observed. Now for CWT correlation is calculation between selected window and signal under observation. Steps involved are as follows

1. Window or wavelet is placed at starting point of the signal. Most compressed wavelet should be selected i.e. $s=1$
2. Wavelet multiplication with signal should be carried out. Integrate the result overall time and then multiplied with factor $\frac{1}{\sqrt{|s|}}$ for uniform energy distribution
3. Shift the wavelet and calculate correlation value for this shifted time and scale 1
4. Above procedure needs to be perform till last point of the signal
5. Increase the value of scale and perform all the above bulleted steps
6. Each calculation will give a correlation value which fill rows of cwt plots

7. CWT is obtained after calculating all s values

4.4.3 Results Obtained Using CWT

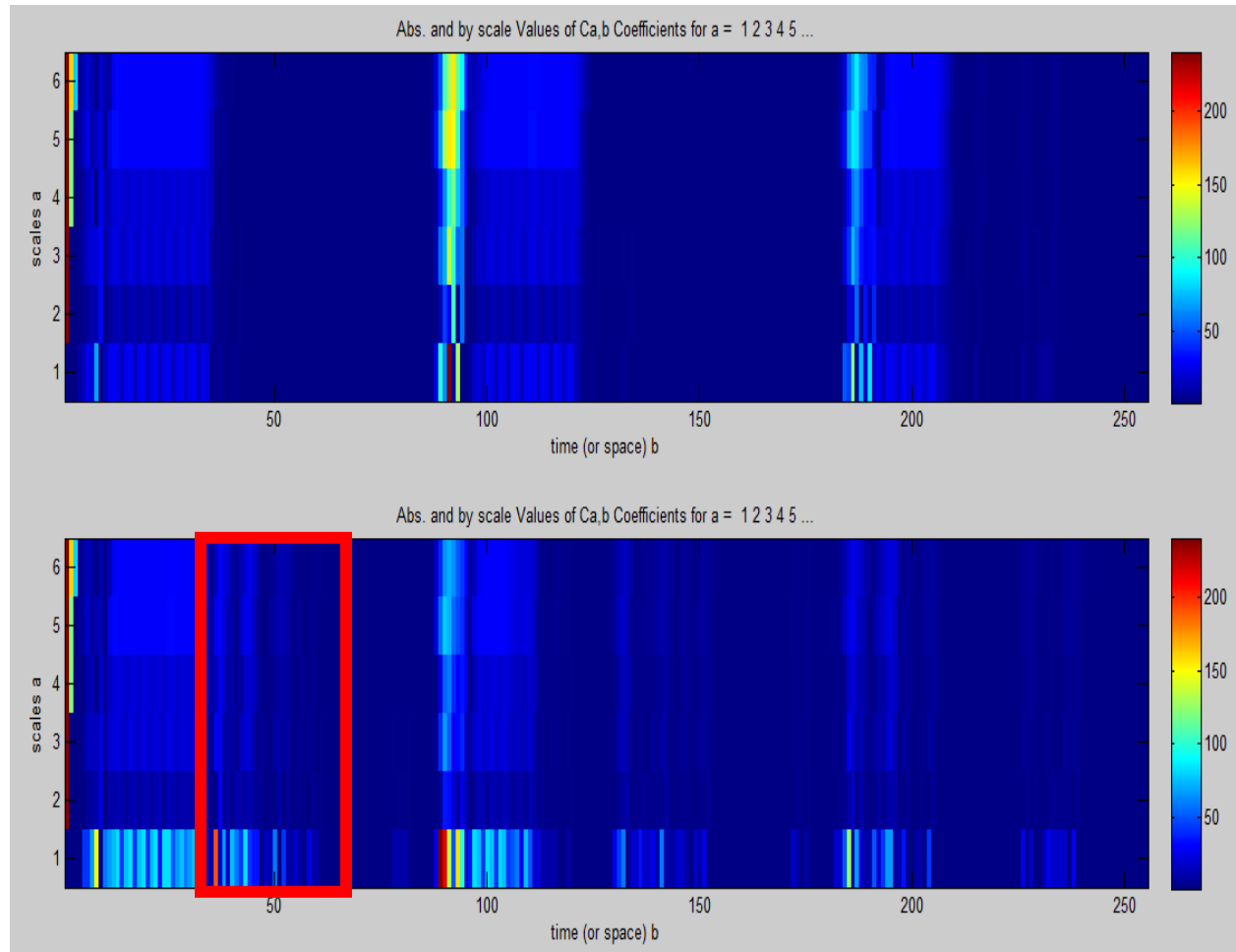


Figure 4-11: Wavelet Spectrum of Healthy and Cracked Location. Top is Healthy Location Wavelet Spectrum and Bottom is Cracked Location Wavelet Spectrum

Figure 4-11 is result obtained using CWT with the help of 'Haar' window with '6' scale levels. Figure 4-11 is comprises of two images first one is of location where we don't have any crack and second is of cracked location. Red rectangular box is drawn to highlight the difference between two locations. It is also observable from CWT result that at scale '1' i.e. most compressed Haar wavelet, prominent difference between crack and without crack location can be observed.

Figure 4-12 mentions the CWT result of two cracked location with same parameters as used previously. This clearly shows that we have crack at two different locations. It is also necessary to mention that the maximum correlation value occurs when we use most compressed wavelet means at scale value 1

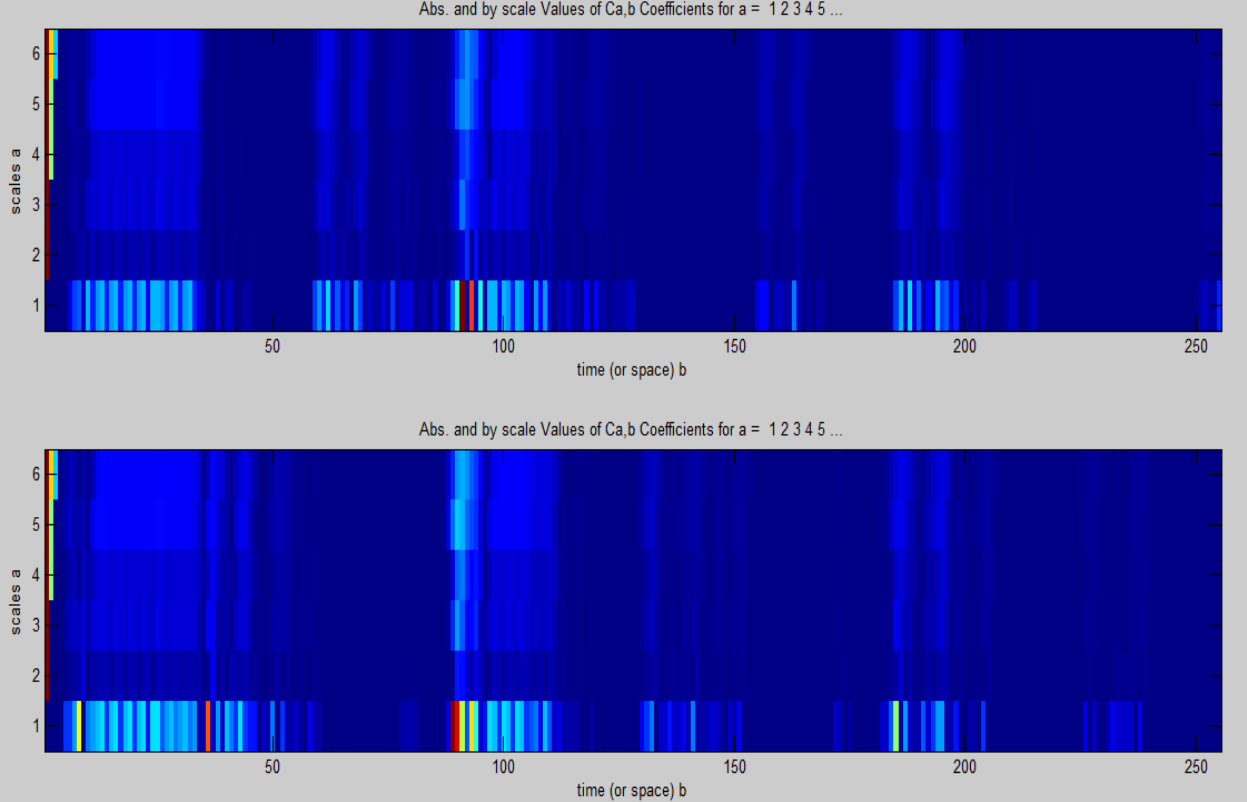


Figure 4-12: Wavelet Spectrum of Cracked Locations

Figure 4-11 and Figure 4-12 mentions the CWT result which is the total value of CWT coefficients. These coefficients can also be viewed separately for each point. There are total of six coefficients plots that can be extracted from a single CWT plot of a either healthy or either

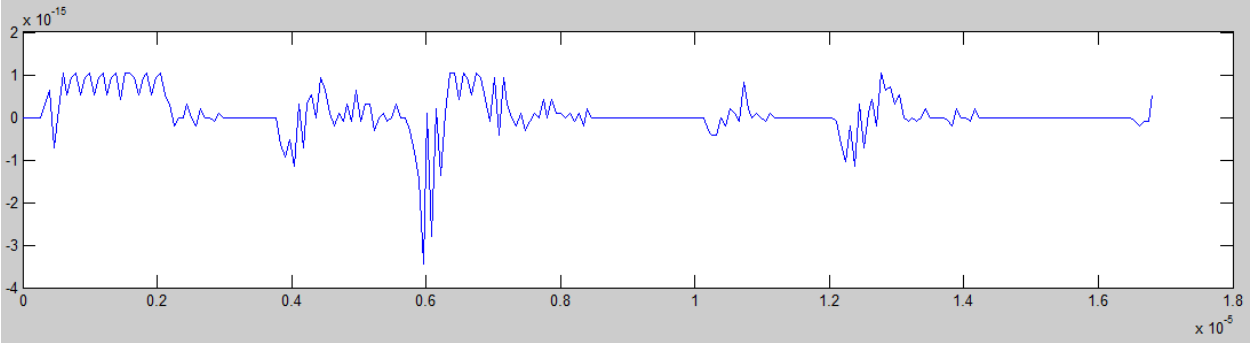


Figure 4-13: Cracked Location Coefficient Plot at Scale Value 1 using Haar Wavelet

unhealthy location. Figure 4-13 and Figure 4-14 shows the 1st Coefficient of CWT from cracked and healthy locations using 6 point Haar wavelet

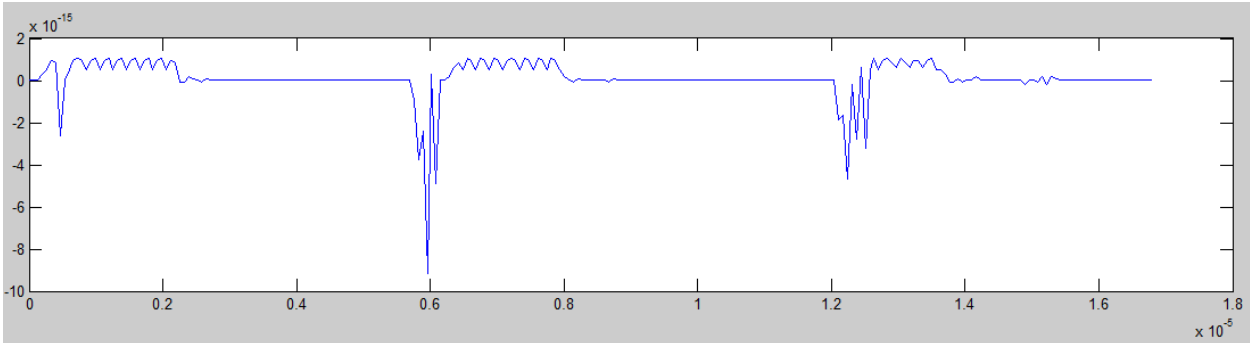


Figure 4-14: Healthy Location Coefficient plot with Scale Value 1 using Haar Wavelet

4.5 Discrete Wavelet Transform

Discrete wavelet Transform doesn't mean discrete version of CWT. Discrete Wavelet Transform is based on a concept of Sub Band Coding which was firstly developed for speech signals. DWT gives a good result for analysis while consumes lesser computational time. Before providing the

results it is necessary to give some details about sub band coding and algorithms for DWT. DWT is also termed as decimated wavelet transform

4.5.1 Sub Band Coding

In CWT correlation was computed by using scale for analyzing window, shifting the signal in time, multiplying signal with the wavelet and integrating over all times. Most important parameters were translation and scaling while dealing with CWT. In DWT filters of different cut off frequencies are used to compute DWT analyzed signal coefficients. High pass and Low pass filters are used to observe high and low frequency components of the signal

Up-Sampling and Down-Sampling is used which changes the scale of the signal whereas filtering operation changes the information part of the signal means its resolution. Up Sampling by factor 2 refers to adding new sample value between two sample values of the signal and down samplings refers to dropping every other sample value. DWT decomposes the signal into coarse approximation and detail information. The decomposition of the signal into different frequency bands can be obtained by high pass and low pass filtering operation. High pass and Low Pass filtering is associated with scaling and wavelet functions respectively

Filtering operation can mathematically be expressed as

$$y_{high} = \sum_n x[n] \cdot g[2k - n]$$

$$y_{low} = \sum_n x[n] \cdot h[2k - n]$$

At each level time resolution becomes half and frequency resolution doubles due to filtering and sub sampling operation. This procedure of sampling and filtering is known as Sub Band Coding

Figure 4-15 mentioned below illustrates this procedure, where $x[n]$ is the original signal, $h[n]$ and $g[n]$ are low pass and high pass filters, respectively. The frequency of the signal at each level is marked as 'f'

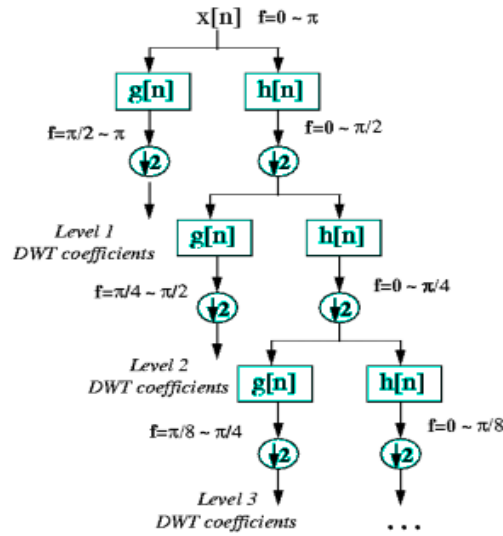


Figure 4-15: DWT Filtering

4.5.2 DWT Result

Below mention is the figure of cracked location A-Scan with detail coefficient at level 1 using Haar window

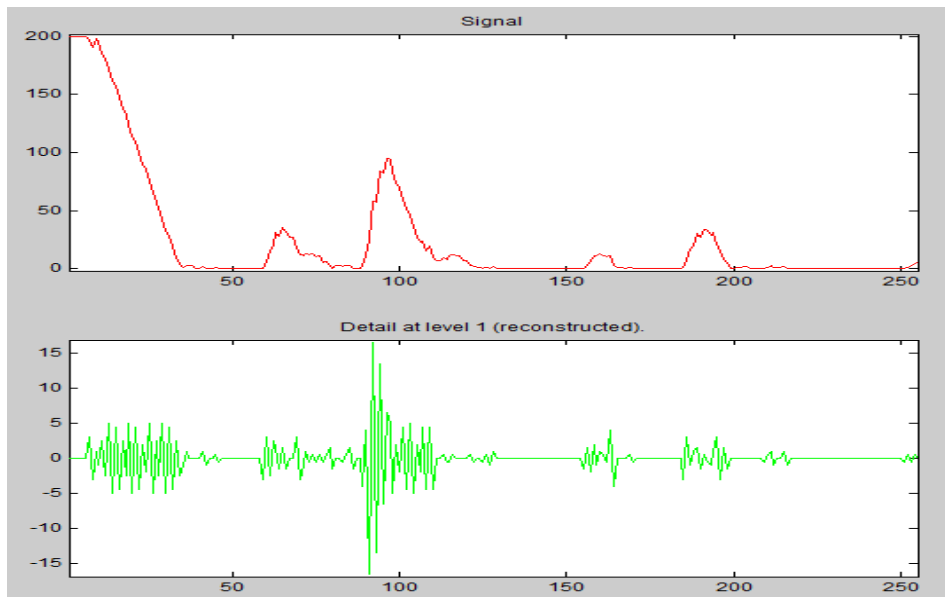


Figure 4-16: DWT Co-efficient

Below mention is the detail coefficient obtained using Haar Window based on DWT at healthy location

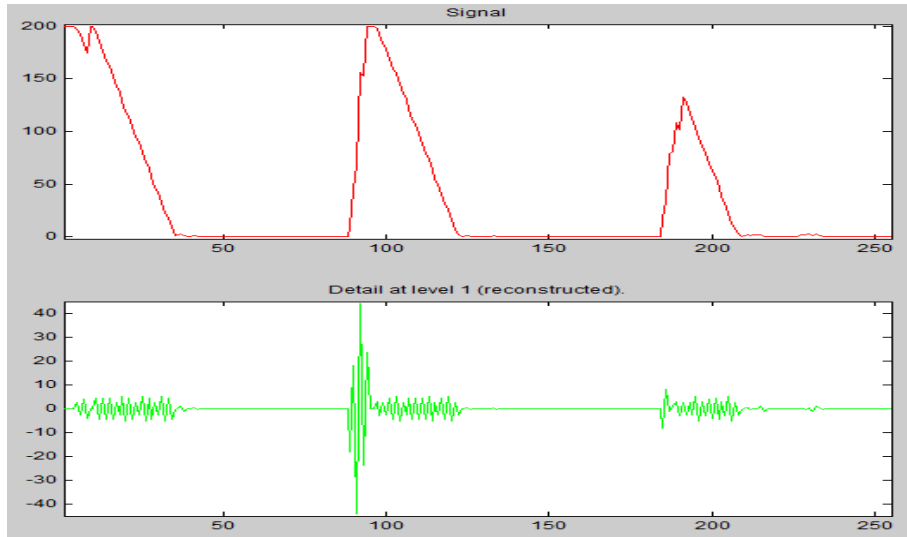


Figure 4-17: DWT Level 1 Coefficient Healthy

Complete result of DWT for 3 levels DWT with coarse approximation and details coefficients

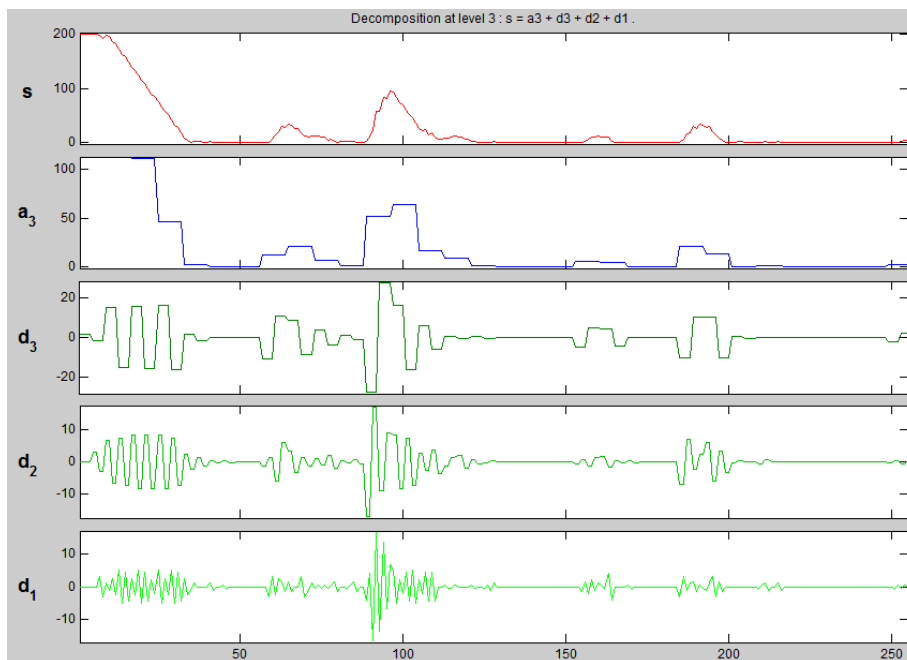


Figure 4-18: Complete DWT Result

4.6 Stationary Wavelet Transform

Stationary wavelet transform is also termed as un-decimated discrete wavelet transform. This is primarily used for noise reduction in signal processing. The main reason behind this is signal reconstruction or synthesis as in case of DWT if it requires to re-construct signal from decomposed signal it gives poor result. Further there is another issue of shift invariance with DWT. SWT also don't have any aliasing problem further in SWT filtering both high pass and low pass is done at each level.

Below mention is the result of SWT coefficients obtained at cracked location 25

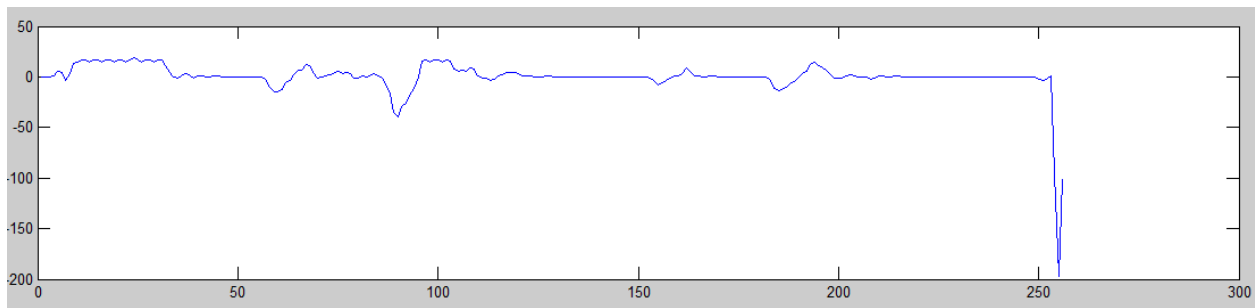


Figure 4-19: SWT Coefficient at Cracked Location

Below mentioned is the SWT coefficient obtained at location where we don't have any crack

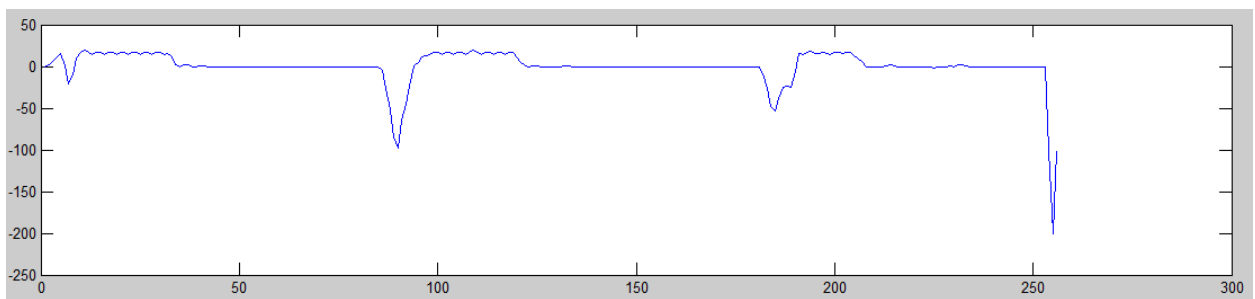


Figure 4-20: Healthy Location SWT Coefficient

From the above two plots it is easily deduced that these are having no noise as compared to the plot obtained with decimated wavelet transform or DWT. Signal re-construction is not required for UT NDT till yet so it is of lesser use

One important difference between CWT and DWT is of scaling. In DWT or SWT down sampling is done based on analysis which was also referred as scaling where in case of CWT scaling is done on each and every point so this is the main logic of calling CWT as continuous . While using with software discrete continuous wavelet transform is used.

STFT and Wavelet Transform are not sufficient while extracting features from non-linear and non-stationary signals. STFT and WT support non stationary signal's feature extraction but when it comes to non-linear these both transform assumes the signal as linear for the portion of window. This assumption of linearity makes these two transform results insufficient as A-Scan signal is non-linear in nature. STFT and Wavelet needs priori basis in the shape of window to analyze signals. This also reduce the originality of the result due to difference in shape and characteristics of original signal as compare to the window shape. In order to overcome the short comings of STFT and WT , Hilbert Huang Transform is used in this research to get energy based characteristics of the original signal without making some assumption regarding linearity and basis of the signal . HHT is empirical method and used directly on A-Scan data. HHT has proved its importance in many areas. In next chapter HHT is described in detail and its useful results are obtained and presented to evaluate energy based characteristics of the non-linear and non-stationary A-Scan signal obtained from aircraft structure test specimen

5 FLAW CHARACTERIZATION USING HILBERT HUANG TRANSFORM

5.1 Introduction

Hilbert Huang Transform, was proposed by Professor Huang et al[13] , for non-linear and non-stationary signal analysis . The HHT has been explored in the applications of structural health monitoring, medical imaging, radar, speech, under-water acoustic feature extraction and climate variation analysis [14-20]. In research of gravity wave for black holes, HHT is used by NASA. It has been shown that HHT can be successfully utilized in many application areas, although there are still some critical mathematical problems to be solved [21].

5.2 HHT Standard Process:

There are two fundamental processes involved in HHT, Empirical Mode Decomposition (EMD) and Hilbert spectral Analysis (HSA). Empirical mode decomposition results in Intrinsic Mode Functions (IMFs) and Hilbert spectrum which shows the energy and time-frequency is obtained by evaluating Hilbert Transform of each IMF.

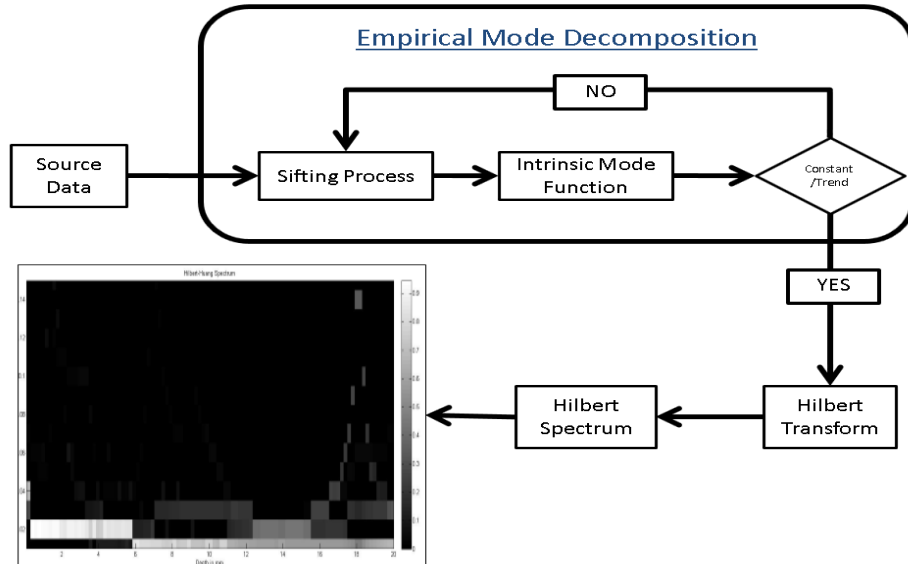


Figure 5-1: Flow Graph for Hilbert Huang Transform Process

5.2.1 Empirical Mode Decomposition:

The purpose of EMD is to decompose a time domain signal $x(t)$ into series of intrinsic mode functions (IMFs), with the help of sifting process. IMFs are obtained by calculating local characteristics of the original signal. Local information of signal includes location of local maxima, local Minima and zero crossing points. Frequency of IMF is the function of time which makes them suitable for time-frequency representation. Sifting process is used to decompose time domain signal (in our case, A-Scan) into series of IMFs

Mathematical representation of EMD is mentioned below

$$x(t) = \sum_{i=1}^N IMF_j(t) + r_1(t) \quad (5-1)$$

Where, $r_1(t)$ is signal residue and $IMF_j(t)$ represents j th IMF. In order to select an IMF, it is mandatory for $H_k(t)$ to satisfy two conditions. Firstly, number of zero crossings and number of extrema are equal or may differ by one. Secondly, the mean value $m(t)$ should be zero. IMF are obtained by a process called as sifting process or EMD.

5.2.2 Steps Involved in EMD Calculation:

Steps involved in this sifting process are as follows:

- I. Calculation of Local Maxima and Local Minima points from signal $x(t)$ with the help of cubic spline interpolation to make upper envelop $U(t)$ and lower envelop $V(t)$

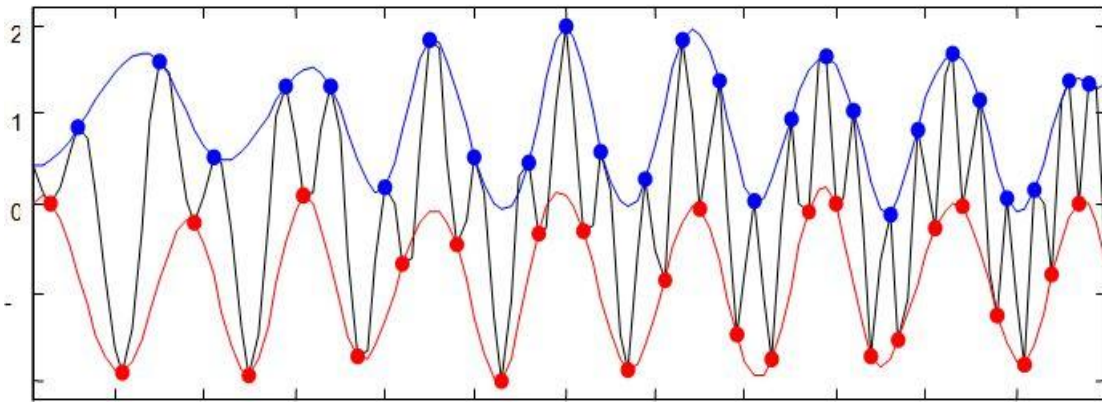


Figure 5-2 : Signal with marking of Upper Envelop (blue) and Lower Envelop (Red)

- II. Calculation of Average Value (mean) from upper and lower envelop obtained in Step I

$$m(t) = \frac{U(t)+V(t)}{2} \quad (5-2)$$

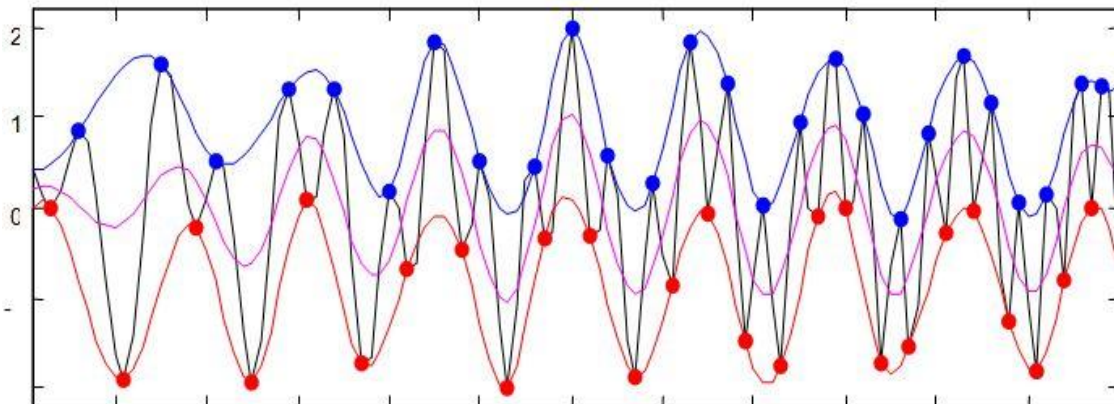


Figure 5-3 : Mean Value Calculation. Curve mentioned in Pink is plot of mean values

- III. Calculation of first IMF, $H_k(t) = x(t) - m(t)$, check if it satisfies IMF conditions.

Incase both conditions of IMF fulfilled go to step IV or otherwise select $x(t) = H(t)$ for next iteration

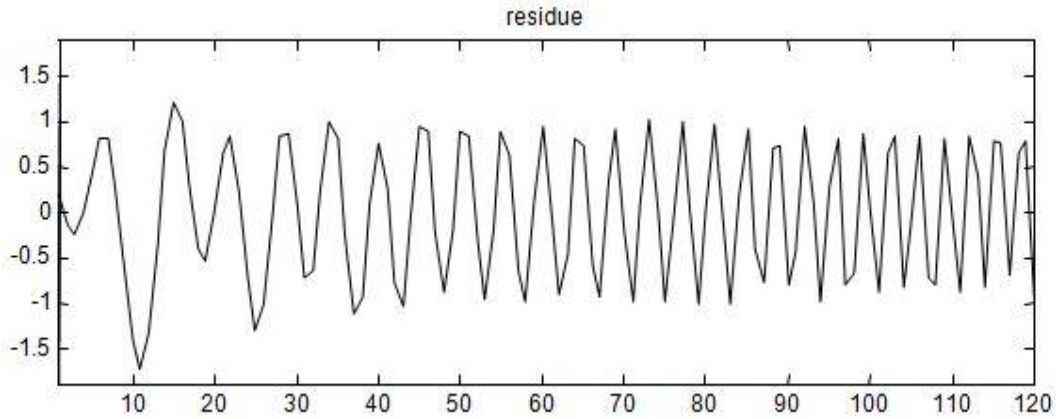


Figure 5-4 : Residue Plot, obtained after subtracting mean value from original signal

- IV. Select the IMF: $H_1(t)$ is the first IMF i.e. $IMF_1(t)$. Now, update iteration index, $= i + 1$, subtract selected IMF from original signal and use subtracted signal for next IMF calculation i.e. $x_1(t) = x(t) - IMF_i$
- V. Calculate residue from step IV, if it is a constant or monotonic function, save all IMFs. If it is not residue, go back to step I. Monotonic or constant function extraction from original signal for completion of EMD is termed as stoppage criteria for the whole process

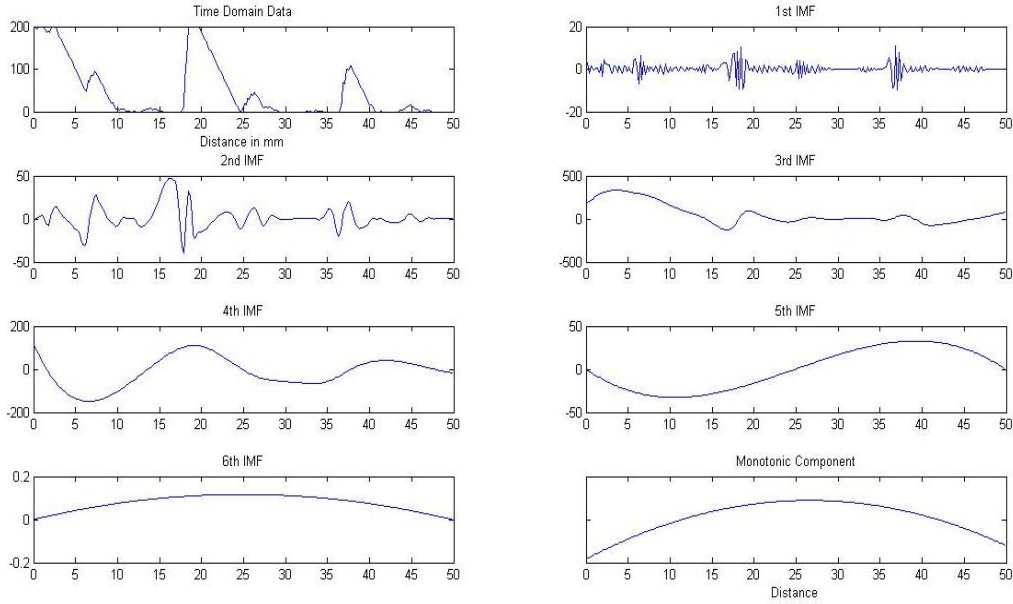


Figure 5-5 : IMF plots using EMD Process

5.3 Hilbert Transform

Hilbert Transform, is a signal processing technique used to calculate analytical signal. Hilbert Transform produces a function $H(u)(t)$ if applied to signal $u(t)$ in same domain. The Hilbert transform is linear operator in mathematics and named after David Hilbert. Hilbert operator was first introduced for solving Riemann-Hilbert Problem of holomorphic function. Originally Hilbert Transform was defined for periodic or functions lies on the circle, convolution of Hilbert Kernel with the signal results in Hilbert Spectrum.

The Hilbert transform of any signal $u(t)$ can be evaluated with the help of convolution of signal

with the function $h(t) = \frac{1}{\pi t}$

Mathematically, the Hilbert transform of a signal $u(t)$ is given by

$$H(u)(t) = p.v. \int_{-\infty}^{\infty} u(\tau) h(t - \tau) d\tau = \frac{1}{\pi} p.v. \int_{-\infty}^{\infty} \frac{u(\tau)}{t - \tau} d\tau$$

$H(u)(t)$ Can be used for calculation of instantaneous frequency

$$\text{Inst. Frequency} = \frac{1}{2\pi} \frac{d\theta}{dx}, \quad \text{Where } \theta = \tan^{-1} \frac{H(u)(t)}{u(t)}$$

Figure [] shows the sample hilbert spectrum obtained at some location

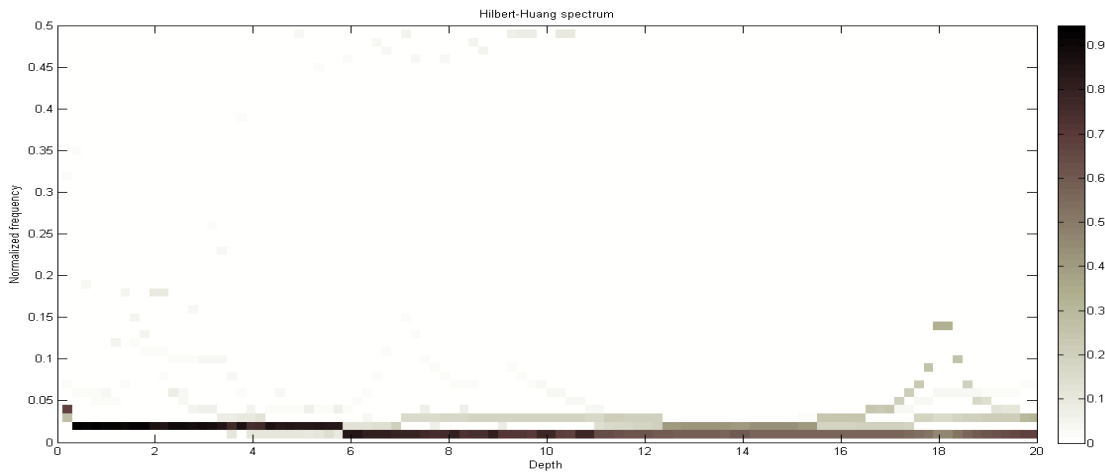


Figure 5-6: Hilbert Huang Spectrum

5.4 Data Acquisition for HHT

Ultrasonic testing for Hilbert Huang Transform is carried out on test piece made of same material as that of Fuselage of the Aircraft with machined drilled flaws. Figure 5-7 shows the schematic of test specimen with front, top and side views. The area is also marked from where UT data was acquired. There were three artificial flaws developed on this test piece. Data was acquired and stored using UT equipment. Data format analysis is carried out and A-Scans (time domain signal) are reproduced using plotting tools in MATLAB. Test specimen was of 19 mm of thickness. At depth of 8-mm three cracks were drilled at different locations. Dimensions of the crack are tabulated in Table 5-1

Table 5-1: Crack Dia. Dimensions

Dia. Of Circular Cracks at 8-mm Depth		
3 mm	4 mm	5 mm

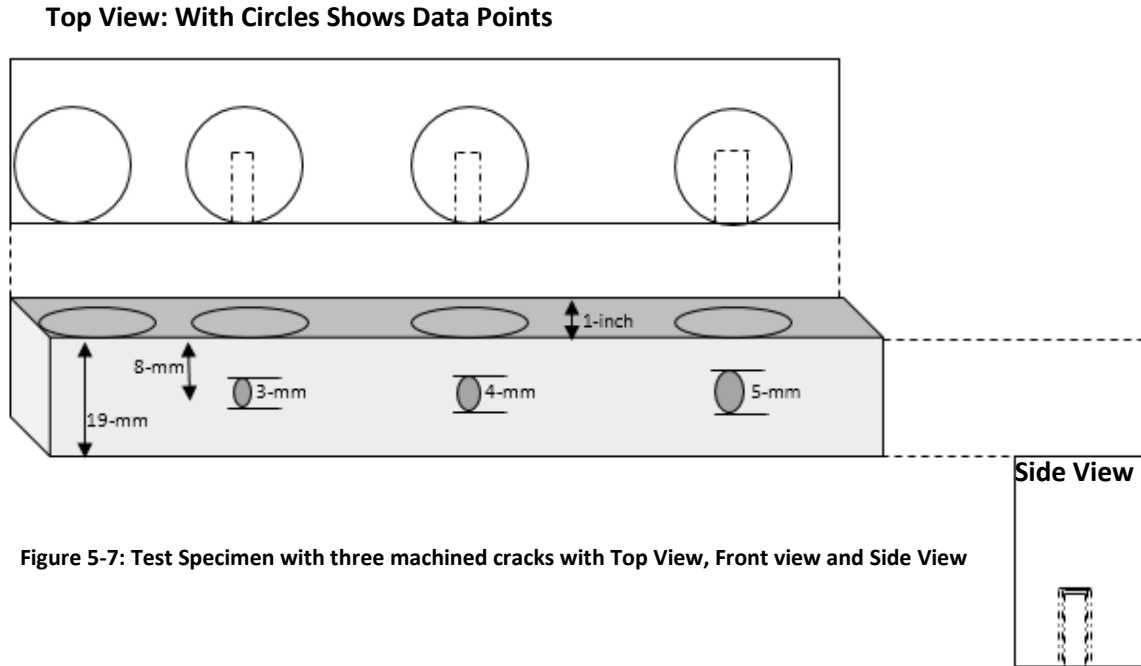


Figure 5-7: Test Specimen with three machined cracks with Top View, Front view and Side View

Data was acquired using serial communication between PC and UT equipment Masterscan Sonatest 350M. Data format analysis algorithms were developed, as the obtained data includes headers which is the information about the software/firmware version and model of the equipment. Headers were removed using developed algorithms in MATLAB, and A-Scans are then reproduced to evaluate the results. Figure 2 shows the A-Scans plot of healthy and cracked location. Figure 5-8(a) is the plot of A-scan acquired at healthy (without crack) location whereas Figure 5-8 (b), (c) and (d) are A-Scans obtained at cracked locations. As evident, flaw characterization is difficult using time domain signals. Ultrasonic signals are non-linear and non-stationary in nature, therefore Hilbert Huang Transform is applied on these signals (A-Scans) to obtain flaw characterization features.

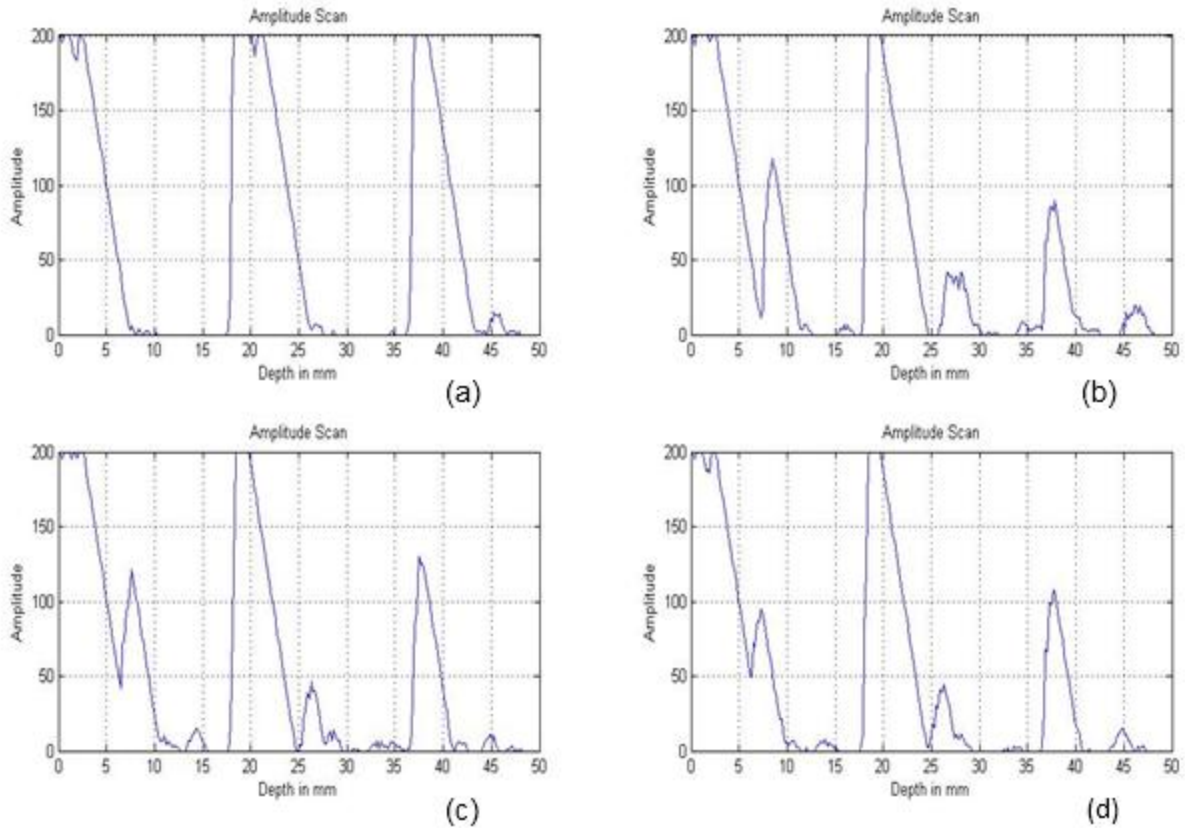


Figure 5-8: A-Scans Plot of Healthy and Cracked Location. (a) Healthy Location. (b) Cracked Location having Crack of 3-mm. (c) Cracked Location having Crack of 4-mm. (d) Cracked Location having crack of 5-mm

5.5 HHT Results and Discussion

HHT was applied on A-Scan data of test specimen with cracks at three different locations as tabulated in Table 5-1. In the first step, EMDs were obtained applying HHT algorithms using sifting process. Figure 5-9 and Figure 5-10 shows the EMD or IMFs of A-Scans acquired from healthy and cracked locations. Total of six IMF plots are obtained from each A-Scan of the inspected location. In the second step, Hilbert Spectrum is evaluated from these IMFs to obtain time-frequency and energy distribution plots.

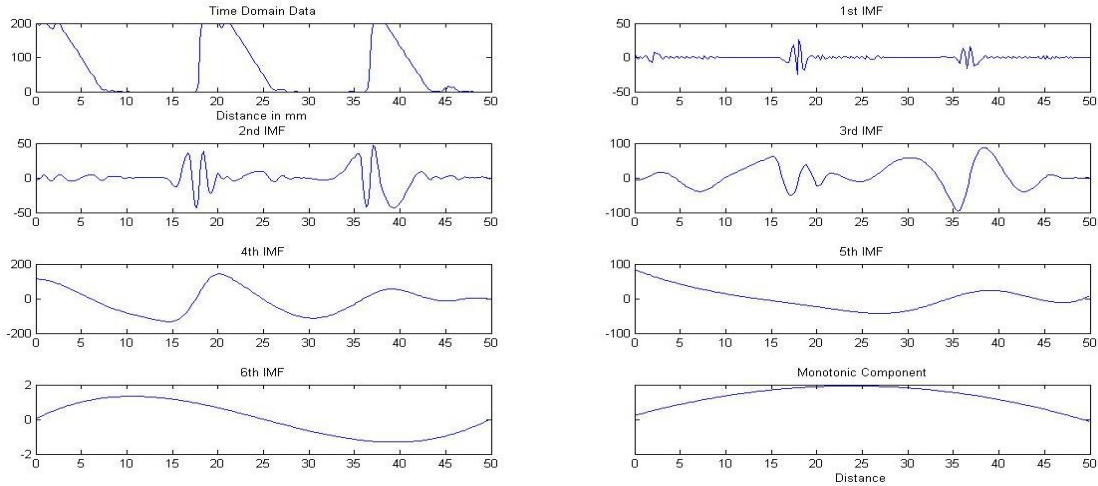


Figure 5-9: Healthy Location IMFs

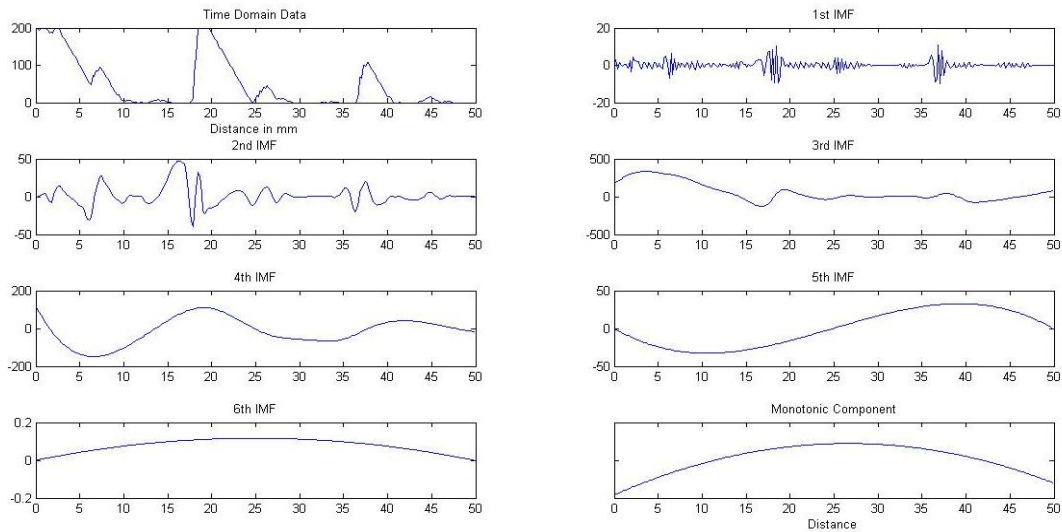


Figure 5-10: Cracked Location IMFs, Crack of 5-mm dia. at depth of 8-mm

IMFs are obtained at each cracked location. IMFs pertaining to 5-mm crack location and healthy locations are shown in Figure 5-9 and Figure 5-10 respectively. The figures highlight the difference between IMFs computed from A-scans acquired from healthy and cracked location. Hilbert Spectrum is then obtained using IMFs of A-Scans acquired at different locations. Figure 5-11 shows the Hilbert Spectrum pertaining to healthy and cracked locations.

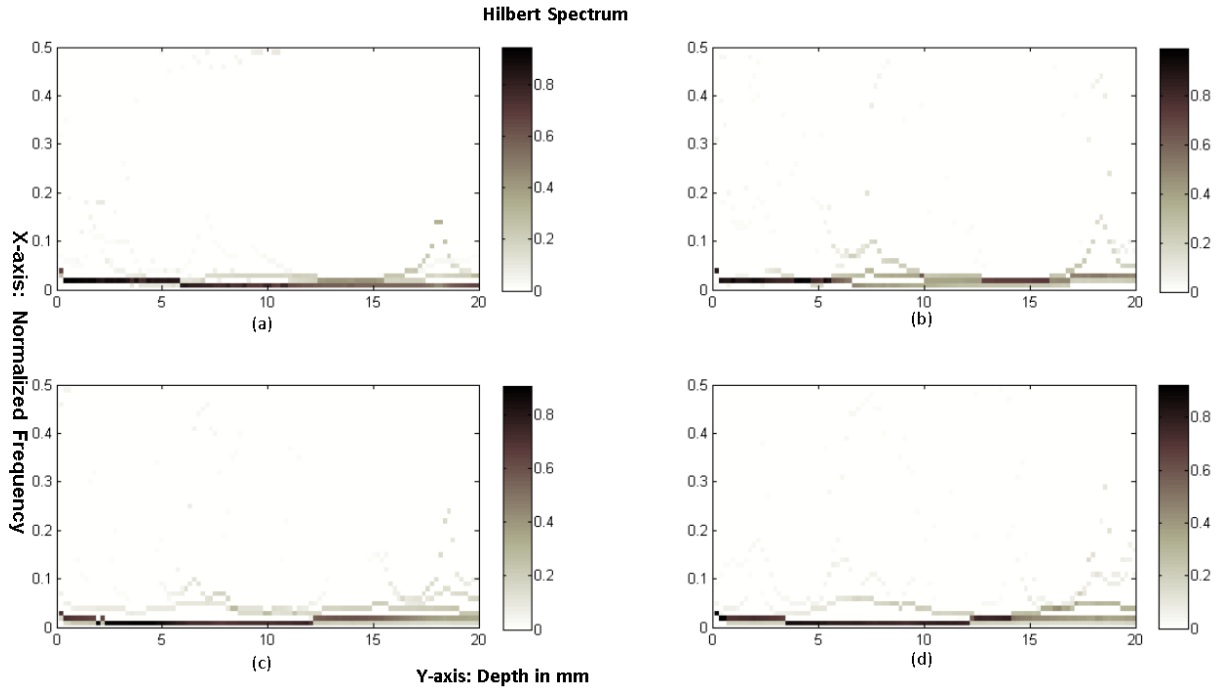


Figure 5-11: Hilbert Spectrum. (a) Healthy Location. (b) Cracked Location, crack of 3-mm dia. (c) Cracked Location, crack of 4-mm dia. (d) Cracked Location, Crack of 4-mm dia.

Hilbert Spectrum's zoomed view is shown in Figure 5-12. A gated Region of interest (ROI) is selected between 6-mm till 10-mm on x-axis with a normalized frequency range between 0.04 till 0.1 Normalized frequency band on y-axis. This selection is made after analyzing the overall spectrum at each location. It was observed that the gated ROI offers energy concentration wherever there are cracks.

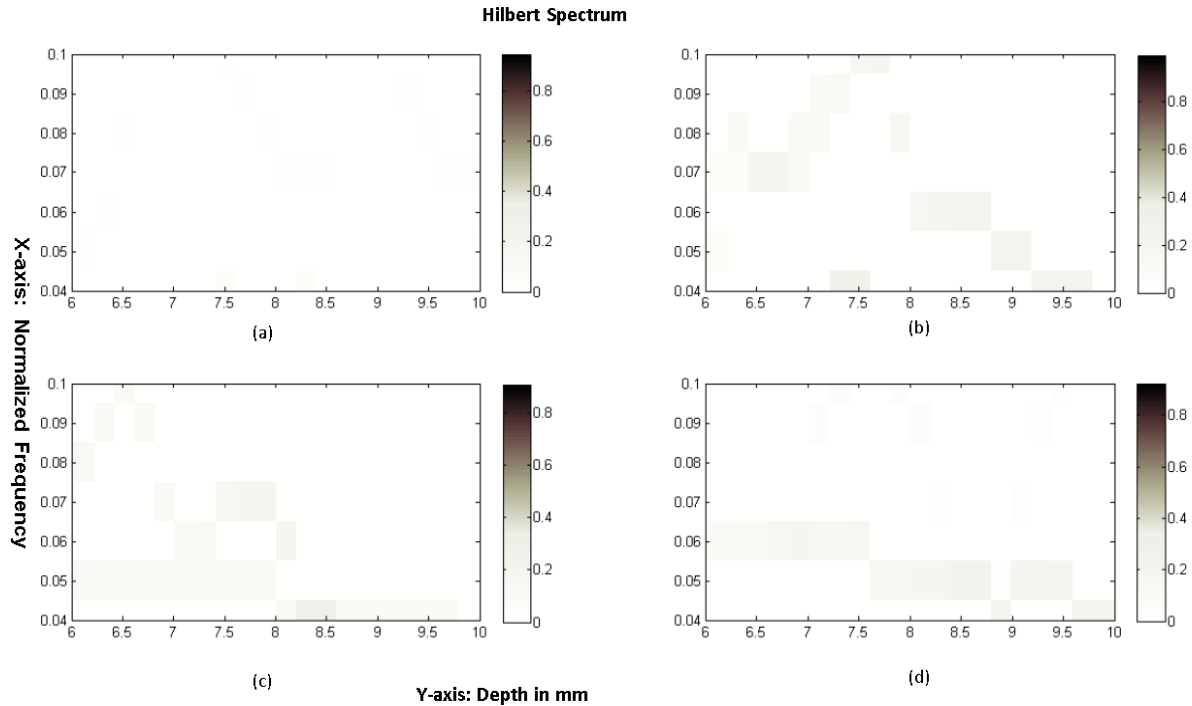


Figure 5-12 : ROI HHT Spectrum of each Location. (a) Healthy Location. (b) Cracked Location, crack of 3-mm dia. (c) Cracked Location, crack of 4-mm dia. (d) Cracked Location, Crack of 4-mm dia.

Figure 5-12 plots are the Hilbert Spectrums obtained from the test data. The Hilbert spectrums show time-frequency and energy distribution of signals acquired from cracked and healthy locations. It can easily be observed that there is no energy between selected depth readings i.e. between 6 mm till 10 mm as there was no crack in Figure 5-8 (a). Some visible changes in energy distribution at and near to the cracked locations can be observed. In order to profile the crack based on HHT spectrum plot, energy is integrated in the region of interest to establish the relationship between flaw size and energy concentration in particular bands. Table 5-2 shows the summation of the energies concentrated in normalized frequency bands (0.04-0.1) around cracked dimensions. This clearly indicates more energy is concentrated in frequency bands of interest around larger sized cracks.

Table 5-2: Energy Distribution between 6 mm till 10 mm depth of Specimen

Normalized Frequency Band 0.04-0.1)	Healthy Location	Cracked Locations dia.		
		3 mm	4 mm	5 mm
Energy (6-10mm depth)	0	0.0149	0.0168	0.0203

A relationship can be established between the energy concentrated in the window formed by frequency band of interest at the particular location and the flaw size (area). Thus computing the concentrating energy in the region of interest would offer the flaw profile

CHAPTER 6

6 CONCLUSION AND FUTURE WORK

6.1 Conclusion

Ultrasonic testing is used to detect and classify flaws on aerospace structures using modern signal processing techniques. Flaw diagnosis algorithms have been developed and subsequently implemented on the raw data acquired from actual aircraft structures. Time frequency analysis is conducted, due to non-stationary and non-linear nature of acquired ultrasonic signals from Aerospace structures. Hilbert Huang Transform is then applied for flaw detection and characterization. Intelligent feature extraction based on energy-frequency distribution at particular locations for diagnosis and crack estimation with the help for Hilbert Huang Transform is suggested in this Thesis.

Feature based on Hilbert Huang Transform offers a reliable mean for detection and characterization of cracks / flaws in aircraft structures

6.2 Future Work

Future efforts can be utilized to get more sophisticated results regarding flaw dimensions with the help for UT NDT using multiple transducers. Efforts can also be utilized to apply Hilbert Huang Transform to more complex data acquire from aircraft structure using modern UT equipment's. Prognosis study can also be initiated with the help of current data and results to properly estimate remaining useful life of the aircraft structure which can help to plan repair and replacement schedule efficiently

References

1. Polikar, R., Udpa, L., Udpa, S.S. and Taylor, T (1998). "Frequency invariant classification of ultrasonic weld inspection signals." *Ultrasonics, Ferroelectrics and Frequency Control, IEEE Transactions on* 45(3): 614 - 625.
2. Z. Feng, M. J. Z. a. X. W. (2006). *Ultrasonic Signal Signatures for Pipeline Damage Identification*. Edmonton, Alberta T6G 2G8 Department of Mechanical Engineering, University of Alberta
3. SHOKOUHI, P., GUCUNSK, N. and MEHER, A. (2006). *Time-Frequency Techniques for the Impact Echo Data Analysis and Interpretations*. 9th European NDT Conference (ECNDT). Berlin, Germany, ECNDT.
4. Petculescu, P., Zagan, R., Prodan, G. C. and Danisor, A. (2005). "Ultrasonic spectroscopy based on wavelets transform for materials characterization." *ROMANIAN JOURNAL OF PHYSICS* 50(8): 701-710.
5. C. J. Brotherhood, B. W. Drinkwater and R. J. Freemantle, 2003, *An ultrasonic wheel-array sensor and its application to aerospace structures*, *Insight Vol 45 No 11 November 2003*, pp 729-734.
6. *Non Destructive Testing Handbook, third edition: Volume 7, Ultrasonic Testing*. American Society for Non Destructive Testing
7. H. Speckmann, R. Henrich, *Structural Health Monitoring - Overview on technologies under development*, *Proc. of the World Conference in NDT, Volume 9, No 11, (2004)*
8. S. G. Sampath, *Aging combat aircraft fleets-long term applications*, (Neuilly-surSeine/France: AGARD LS-206), (1996)
9. R. Radhakrishnan, *Damage Characterization*, Joint FAA/Delta 8th Quarterly Meeting, *Destructive evaluation and extended fatigue testing of a retired passenger aircraft*, Atlanta, (2004).
10. C. Boller, *Next generation Structural Health Monitoring and its integration into aircraft design*, *Int. J. Sys. Sci., Volume 31, No 11, 1333-49 (2000)*
11. I. N. Komsky, *Modular dry-coupled ultrasonic probes for field inspections of multi-layered aircraft structures*, *Proc. SPIE, Volume 5768, 176 (2005)*
12. H. J. Schmidt and B. Schmidt-Brandecker, *Structure design and maintenance benefits from health monitoring systems*, *Proc. 3 rd Int. Workshop on Structural Health Monitoring, Stanford, USA, 80-101 (2001)*
13. C. Boller, *Ways and options for aircraft structural health management*, *Smart.Mater. Struct., Volume 10, 432-40 (2001)*

14. Huang, N. E.; Shen, Z.; Long, S. R.; Wu, M. C.; Shih, H. H.; Zheng, Q.; Yen, N. C.; Tung, C. C.; Liu, H. H. (1998). "The Empirical Mode Decomposition and the Hilbert Spectrum for Nonlinear and Non Stationary Time Series Analysis" . Proceedings of the Royal Society of London
15. N.Huang,andN.Attoh-Okine, "TheHilbert-Huangtransformin engineering," CRC Press, Taylorand Francis PublishingGroup,2005.
16. A. Gallix, J.M. Górriz, , J. Ramírez, I.A. Illán, E.W. Lang. "On the empirical mode decomposition applied to the analysis of brain SPECT images", Expert Systems with Applications, Volume 39, Issue 18, 15 December 2012, Pages 13451–13461
17. Ming-Chya Wu, Jeffrey G. Forbes, Kuan Wang, "Cross-correlation analysis to salt-bridge dynamics in force-induced unfolding of titin kinase", 2011 21st International Conference on Noise and Fluctuations, 978-1-4577-0192-4/11/
18. Donghoh Kim, Minjeong Park, and Hee-Seok Oh, "Bidimensional Statistical Empirical Mode Decomposition", IEEE SIGNAL PROCESSING LETTERS, VOL. 19, NO. 4, APRIL 2012
19. J.C. Nunes*, Y. Bouaoune, E. Delechelle, O. Niang, Ph. Bunel, "Image analysis by bidimensional empirical mode decomposition", Image and Vision Computing 21 (2003) 1019–1026
20. ZhiyuanShen, Naizhang Feng, Yi Shen, Member, IEEE, and Chin-Hui Lee, Fellow, IEEE, "A Ridge Ensemble Empirical Mode Decomposition Approach to Clutter Rejection for Ultrasound Color Flow Imaging", IEEE TRANSACTIONS ON BIOMEDICAL ENGINEERING, 2011
21. G.Ge, E.Sang, Z.Liu and B.Zhu,"Underwater acoustic feature extraction based on bi-dimensional empirical mode decomposition in shadow field," IEEE Proceedings of signal design and its applications in communications, pp.365-367,September2007
22. Yu feng Lu , Oruklu, E. ; Saniie, J."Application of Hilbert-Huang transform for ultrasonic nondestructive evaluation".IEEE International Ultrasonic Symposium Proceedings